universe

IMPACT FACTOR 2.6

CITESCORE 5.2

Article

Noncommutative Bianchi I and III Cosmology Models: Radiation Era Dynamics and γ Estimation

Gil Oliveira-Neto and Yuri Soncco Apaza

MDPI

https://doi.org/10.3390/universe11120408

universe

MDPI

Article

Noncommutative Bianchi I and III Cosmology Models: Radiation Era Dynamics and γ Estimation

Gil Oliveira-Neto * and Yuri Soncco Apaza

Departamento de Física, Instituto de Ciências Exatas (ICE), Universidade Federal de Juiz de Fora, Juiz de Fora CEP 36036-900, MG, Brazil; sonccoapaza.yuri@estudante.ufjf.br
* Correspondence: gilnetojf@ufjf.br

Abstract

In this work, we analyze the dynamical evolution of locally rotationally symmetric anisotropic cosmological models of Bianchi type I (flat curvature) and Bianchi type III (open curvature) within a noncommutative phase space framework characterized by a deformation parameter γ. Using a Hamiltonian formulation based on Schutz's formalism for a perfect radiation fluid, we introduce noncommutative Poisson brackets that allow for geometric corrections to commutative dynamics. The resulting equations are solved numerically, which allows for the study of the impact of γ and the energy density C on the expansion of the universe and the evolution of anisotropy. The results show that $\gamma < 0$ improves expansion and favors isotropization, while $\gamma > 0$ tends to slow expansion and preserve residual anisotropy, especially in the open curvature model. It is estimated that the influence of noncommutativity was significant during the early stages of the universe, decreasing toward the present time, suggesting that this approach could serve as an effective alternative to the cosmological constant in describing the evolution of the early universe.

Keywords: anisotropic universe; bianchi models; noncommutative phase space; noncommutative parameter; early universe evolution; hamiltonian formalism; accelerated expansion; isotropization

check for updates

Received: 24 October 2025
Revised: 29 November 2025
Accepted: 7 December 2025
Published: 10 December 2025

Citation: Oliveira-Neto, G.; Apaza, Y.S. Noncommutative Bianchi I and III Cosmology Models: Radiation Era Dynamics and γ Estimation. *Universe* **2025**, *11*, 408. https://doi.org/10.3390/universe11120408

Copyright: © 2025 by the authors. Licensee MDPI, Basel, Switzerland. This article is an open access article distributed under the terms and conditions of the Creative Commons Attribution (CC BY) license (https://creativecommons.org/licenses/by/4.0/).

1. Introduction

Understanding the dynamics of the universe in its early stages remains one of the main challenges of modern cosmology. It is postulated that during its initial moments, when the energy density and spacetime curvature were extreme, the gravitational interaction was quantized [1]. In this quantum-gravitational regime, the geometry of the universe could not be described by classical general relativity but instead behaved as a highly fluctuating structure, resembling a resonant quantum foam, where multiple spatial configurations coexist in superposition [2]. This concept implies that the universe may have begun in an inhomogeneous and anisotropic state, far from the symmetric and uniform picture we observe today. However, over time and driven by mechanisms such as accelerated expansion, this primordial universe would have evolved toward a simpler configuration: homogeneous and isotropic on large scales, as described by the standard Friedmann-Robertson-Walker (FRW) cosmological model [3,4].

In this context, studies on the process of isotropization and how an initially anisotropic universe can evolve into an isotropic one have been widely developed with the aim of reconstructing the history of the early universe and exploring possible imprints of its quantum origin. From a classical perspective, it has been shown that homogeneous

anisotropic models of Bianchi type [5,6] tend to isotropic solutions in the presence of a positive cosmological constant [7] or in the presence of a reduced relativistic gas (RRG) [8]. The same process of isotropization also takes place in Kantowski-Sachs cosmological models filled with a phantom perfect fluid [9] or with a running cosmological constant [10]. Moreover, dynamical investigations of these models have identified various conditions and mechanisms, such as cosmic viscosity, the presence of a radiation fluid, interactions with scalar fields, or even the action of dark energy, that can favor such evolution toward isotropy [11–13]. In the specific case of Bianchi I cosmological models, we may mention several works dealing with the above-mentioned and other aspects of these models. In Ref. [14], the authors investigated how the presence of a viscous fluid influences the isotropization of a Bianchi I model. A nonminimal extension of the Einstein-Maxwell equations was coupled to Bianchi I models in the presence of a magnetic field in Ref. [15]. The authors obtained several exact solutions of the nonminimal system, including those that described isotropization, inflation, and an isotropic de Sitter solution characterized by a 'screening' of the magnetic field as a consequence of the nonminimal coupling. In Ref. [16], the authors considered the effects of the presence of Skyrmes and a positive cosmological constant in two anisotropic cosmologies. They studied Kantowski-Sachs and Bianchi-I universes and determined the conditions for the late time isotropization of both universes. The authors discussed in Ref. [17] the possible description of the big bang–big crunch cosmological singularities crossing in a Bianchi I universe filled with minimally and conformally coupled massless scalar fields. In Ref. [18], the authors studied the effects of a spatially homogeneous magnetic field in Bianchi I cosmological models. They considered three models filled with a spatially homogeneous magnetic field (SHMF) and different matter contents. In the first one, there was just the SHMF, in the second one, an extra dust fluid, and in the third, an extra massless scalar field (stiff matter). They paid special attention to the identification of the initial and final states of these models and the transition between them. Another important application of the study of anisotropic cosmological models has to do with the presence of anomalies in CMB radiation and the low-quadrupole moment of that radiation. These anomalies in the CMB may be explained by plane-mirroring symmetry on large scales. The low-quadrupole moment in the CMB may indicate an ellipsoidal expansion of the universe [19–28]. In the quantum context, research developed within loop quantum cosmology has shown that specific anisotropic models, such as Bianchi I, can undergo isotropization as a natural result of the evolution of the universe in quantum-corrected geometries without the need to impose additional external conditions [29,30]. There are also works that studied Bianchi I cosmological models, at the quantum level, using the formalism of quantum cosmology [31–35].

The Bianchi III model, which represents an anisotropic universe with negative spatial curvature, has been extensively investigated in both classical contexts and modified gravity theories. It has been used to study isotropization mechanisms in anisotropic cosmologies [36], the dynamics of dark energy in general relativity [37], and alternative formulations such as Lyra geometry with quadratic equations of state [38]. Within modified gravity theories, the Bianchi III model has been analyzed in $f(R,T)$ gravity, exhibiting accelerated expansion and non-singular behaviors [39]. Furthermore, quantum extensions of the model have been explored, for instance, within Hořava–Lifshitz gravity and in Bianchi III minisuperspace models coupled to electromagnetic fields, where both canonical classical quantization and Wheeler–DeWitt approaches have been employed [40]. These studies illustrate the use of the Bianchi III metric as a framework for examining anisotropies, isotropization, and cosmic acceleration within different theoretical approaches.

Beyond these classical and modified gravity frameworks, another promising approach involves spacetime noncommutativity, which was first introduced by Snyder in the 1940s

as an attempt to regularize divergences in quantum field theory without breaking Lorentz symmetry [41]. In his proposal, spacetime coordinates ceased to commute, giving rise to a modified geometric structure at tiny scales. Although initially overlooked, this idea experienced a significant resurgence due to developments in string theory, membrane theory, and M-theory, where noncommutativity naturally emerges in specific physical regimes [42–44]. In this new context, spacetime noncommutativity has become the subject of intense investigation, particularly in cosmology. Various studies have shown that noncommutative (NC) effects can profoundly alter the dynamics of the early universe [45–51], even contributing to the elimination of singularities and modifying the expansion process. This suggests that noncommutativity played an active role throughout all stages of cosmic evolution. One of the primary motivations for incorporating this structure into classical cosmological models is the possibility that residual observable effects may persist to the present day.

Consequently, a growing line of research in cosmology involves extending anisotropic models by incorporating NC structures in phase space. This proposal, motivated by advances in string theory and quantum gravity, introduces a parameter γ that deforms the Poisson algebra between dynamical variables. These modifications allow for the exploration of alternative evolutionary trajectories and have been associated with mechanisms that could suppress anisotropies, induce accelerated expansion, or eliminate singularities [45,46]. However, the specific study of the Bianchi I (flat curvature) and Bianchi III (negative curvature) models during the radiation-dominated era within this NC framework remains limited. We may mention Refs. [47,50,51], where NC Bianchi I models are studied. Moreover, to the best of our knowledge, the noncommutative deformation of Bianchi III cosmologies has not yet been explored, providing motivation for its consideration in the present work.

Therefore, this study aims to analyze the dynamical evolution of the locally rotationally symmetric (LRS) NC Bianchi I and Bianchi III cosmological models, coupled to a perfect radiation fluid, investigating the effects of the NC parameter γ on the expansion and isotropization processes. Since we believe noncommutativity was more important during the early stages of the universe, we consider as the matter content of the cosmological model described here a radiation fluid, which was dominant during that period. Our main motivation to choose the LRS version of these spacetimes is the similarities between the metrics. As we shall see later, these similarities will allow us to compare some results coming from Bianchi I and III cosmological models in a simple way. As a matter of completeness, we mention that the LRS version of Bianchi I and III lets the metric of these spacetimes be very similar to the metric of the Kantowski–Sachs spacetime (positive curvature) [52]. Unfortunately, as we shall see later, the Kantowski–Sachs model will not be studied in the present work because it does not produce expanding solutions under the conditions considered here. The parameter γ is introduced due to a deformed Poisson bracket algebra. More precisely, it appears because we introduce four nontrivial Poisson brackets between all geometrical variables and the matter variables of the model. We associate the same NC parameter γ with all nontrivial Poisson brackets. An important difference between the present paper and the Refs. [47,50,51], is that here we use the LRS form of the Bianchi I metric. Also, we may say that the present model is more noncommutative than the one considered in Ref. [50]. This is the case because the authors of Ref. [50] considered only two nontrivial Poisson brackets between the geometrical variables and the matter variables of the model. The content of matter in the model of Ref. [50] is the same as in the present model. On the other hand, the authors in Ref. [51] introduced six nontrivial Poisson brackets and in Ref. [47] four nontrivial Poisson brackets, all just between the geometrical variables of the model. The model in Ref. [51] differs from the present model

and from the ones in Refs. [47,50], because the content of matter there was given by an RRG. Another important difference between the present model and the one in Ref. [51] is the use of the symplectic formalism to introduce the deformed Poisson bracket algebra. Finally, in Ref. [47], the authors solved the dynamical equations in the WKB approximation, while here we solve the complete equations numerically. Besides, they considered a cosmological constant. Additionally, here a quantitative estimation of γ is proposed on the basis of the assumption that the universe has evolved toward a homogeneous and isotropic state at present. This work seeks to evaluate whether noncommutativity may have played a significant role in the early universe and whether its influence can be distinguished from that of commutative models. Furthermore, a systematic comparison was made between the flat (Bianchi I) and open (Bianchi III) models, exploring their differences in terms of sensitivity to the NC deformation. This approach not only enriches the theoretical framework of anisotropic cosmology but may also open new avenues for connecting predictions from NC models with current or future cosmological observations.

Finally, the structure of this work is organized as follows. In Section 2, the Bianchi I and Bianchi III cosmological models coupled to a perfect fluid are introduced, and the superhamiltonian of the models is derived. In Section 3, we define the NC Poisson brackets through the parameter γ, and the equations of motion are obtained in terms of new commutative variables. In Section 4, we consider the case of a radiation fluid. We numerically solve the system of dynamical equations and obtain the behaviors of the scale factor and the anisotropy parameter. We present a detailed study of their various behaviors and a comparison with the commutative case. In Section 5, the parameter γ is estimated from observational data, assuming a homogeneous and isotropic universe. Finally, in Section 6, we discuss and summarize the most relevant results of the paper.

2. The Bianchi Models for Any Perfect Fluid

The LRS line element, which encompasses the spacetimes of Bianchi I (BI), Bianchi III (BIII), and Kantowski-Sachs (KS) [52–56], allows a unified description of such homogeneous and anisotropic universes. Inspired by Misner's parametrization [57], this LRS line element can be expressed as [9],

$$\mathrm{d}s^2 = -N(t)^2\mathrm{d}t^2 + a(t)^2 e^{-\beta(t)}\mathrm{d}r^2 + a(t)^2 e^{\beta(t)}\left(\mathrm{d}\theta^2 + f(\theta)^2\mathrm{d}\phi^2\right). \tag{1}$$

Here, $a(t)$ represents the isotropic scale factor, $\beta(t)$ is the parameter describing anisotropy, $N(t)$ is the lapse function, $f(\theta)$ takes the specific forms: $f(\theta) = \theta$, $\sin(\theta)$, $\sinh(\theta)$, respectively, for the following spacetimes BI, KS, BIII. In the present work, we use *geometrized units* first introduced in Ref. [58]. In these units the speed of light c, Newton's gravitational constant $8\pi G$, and Boltzman's constant κ are all equal to unity. The standard unit, in terms of which everything is measured in this paper, is centimeters. If one wants to recover the standard units, one has to multiply or divide the quantity by a particular factor of unity. For example, if one has a time value in *geometrized units* and wants to obtain it in seconds, one must divide it by the following factor unity: $1.0 = c = 2.997930 \times 10^{10}$ cm/s. For a full list of factors of unity see Ref. [58]. However, in Section 5 we use conventional units to estimate the NC parameter γ. The main motivation to use the *geometrized units* is that we may use time scales and parameter values that allow the numerical calculations and the production of graphics where the behavior of the functions are easily shown. In the metric (1), the anisotropy depends on the parameter $\beta(t)$, which produces differences in the expansion rates along different spatial directions. It is expected that $\beta(t) \to$ constant or zero at late times, implying that the universe, although initially anisotropic, evolves toward an isotropic FRW-like state. It is known in the literature that the Bianchi I and the Kantowski-Sachs

spacetimes tend to the FRW spacetime at late times. However, the Bianchi III spacetime does not reach an exact FRW spacetime at late times. However, it becomes very similar to an FRW spacetime for a period of its evolution [59]. Here, we are going to study the conditions in which the Bianchi III spacetime becomes very similar to an FRW spacetime.

The energy content of the universe can be represented by a perfect fluid. The four-velocity of this fluid, typically expressed as $U^\mu = N(t)\delta^\mu_0$, defines a comoving frame where matter exhibits no spatial motion and evolves only in time. This assumption significantly simplifies the calculations and provides a convenient basis for defining the energy-momentum tensor as

$$T_{\mu\nu} = (\rho + p)U_\mu U_\nu + p g_{\mu\nu}, \tag{2}$$

where ρ represents the energy density, p the pressure, and $g_{\mu\nu}$ is the metric tensor. The equation of state of the fluid is given by

$$p = \alpha\rho, \tag{3}$$

where α is a constant that characterizes the type of fluid.

As we mentioned in Section 1, in the present paper, we introduce the noncommutativities as deformations in the Poisson algebra between the phase space variables of the model. Then, we must write the geometrical and matter Hamiltonians of the model. The Schutz's variational formalism [60] was developed to write the Hamiltonian of a perfect fluid with the equation of state (3). Therefore, in the present paper we use Schutz's variational formalism to write the Hamiltonian of a generic perfect fluid with equation of state (3). In this approach, the four-velocity (U_ν) of the fluid is expressed in terms of six thermodynamic potentials (λ, φ, η, τ, ϑ, s) as follows,

$$U_\mu = \frac{1}{\lambda}\left(\varphi_{,\mu} + \eta\tau_{,\mu} + \vartheta s_{,\mu}\right) \tag{4}$$

where λ is the specific enthalpy, s is the specific entropy, η and τ are associated with the vorticity of the fluid, while φ and ϑ lack a clear physical interpretation in this context. Additionally, the four-velocity must satisfy the normalization condition,

$$U^\mu U_\mu = -1. \tag{5}$$

For these models, which do not assume vorticity, the potentials η and τ vanish. In a comoving coordinate system with the perfect fluid, the expression for U_μ simplifies, and the specific enthalpy λ takes the form of

$$\lambda = N^{-1}(\dot{\varphi} + \vartheta\dot{s}), \tag{6}$$

where the dot means derivative with respect to time t and N is a simplification in the notation of $N(t)$, the lapse function, first introduced in the metric Equation (1).

Considering the equation of state (3), it can be shown by thermodynamic considerations that the pressure in this formalism has the form [61],

$$p = \alpha\left(\frac{\lambda}{\alpha+1}\right)^{1+1/\alpha} e^{-s/\alpha}. \tag{7}$$

This formulation links the thermodynamic properties of the fluid with the dynamical variables in Schutz's formalism.

The action of the theory will be determined by the sum of the Einstein-Hilbert term and the action associated with the perfect fluid, and the total action can be written as

$$S = \int \left(\frac{1}{2} R + \mathcal{L}_{\mathrm{M}} \right) \sqrt{-g}\, \mathrm{d}^4 x \tag{8}$$

where g is the determinant of the metric tensor, R is the Ricci scalar and $\mathcal{L}_{\mathrm{M}}$ is the Lagrangian density of matter, which is equal to the fluid pressure p.

By computing the Ricci scalar R from the metric (1) and substituting p Equation (7), the action takes the explicit form

$$S = \int \left[aN\kappa e^{-\frac{\beta}{2}} - \frac{a^2 \dot{a}\dot{\beta} e^{\frac{\beta}{2}}}{N} - \frac{3a\dot{a}^2 e^{\frac{\beta}{2}}}{N} + \frac{a^3 \dot{\beta}^2 e^{\frac{\beta}{2}}}{4N} + \alpha a^3 N e^{\frac{\beta}{2} - \frac{s}{\alpha}} \left(\frac{\vartheta \dot{s} + \dot{\varphi}}{N(\alpha+1)} \right)^{\frac{1}{\alpha}+1} \right] \mathrm{d}t \tag{9}$$

where $\frac{f''(\theta)}{f(\theta)} = -\kappa$, with $\kappa = 0$ corresponding to the BI model, $\kappa = -1$ to the BIII model, and $\kappa = 1$ to the KS model [53,62].

The Lagrangian density can be obtained from the action of the model Equation (9) and using it, one may write the corresponding superhamiltonian, using the geometrodynamic formulation of general relativity [2],

$$NH = Ne^{-\frac{\beta}{2}} \left(-\kappa a - \frac{P_a^2}{16a} - \frac{P_a P_\beta}{4a^2} + \frac{3P_\beta^2}{4a^3} \right) + Na^3 e^{-\frac{\beta\alpha}{2} + s} P_\varphi^{\alpha+1} \tag{10}$$

where $P_a = -N^{-1} a e^{\beta/2} \left(6\dot{a} + a\dot{\beta} \right)$, $P_\beta = (2N)^{-1} a^2 e^{\beta/2} \left(a\dot{\beta} - 2\dot{a} \right)$, $P_s = \vartheta P_\varphi$, $P_\vartheta = P_M = 0$ and $P_\varphi = a^3 e^{\frac{\beta}{2} - \frac{s}{\alpha}} \left(\frac{\vartheta \dot{s} + \dot{\varphi}}{\alpha M + M} \right)^{1/\alpha}$, are the canonically conjugate momenta of the dynamical variables of the model. The superhamiltonian (10) can be simplified by performing the following canonical transformations [61,63],

$$T = -P_s\, e^{-s}\, P_\varphi^{-(\alpha+1)}, \quad P_T = P_\varphi^{\alpha+1}\, e^{s}, \quad \overline{\varphi} = \varphi - (\alpha - 1) \frac{P_s}{P_\varphi}, \quad \overline{P}_\varphi = P_\varphi. \tag{11}$$

Using the transformations (11) in the matter term of the superhamiltonian (10), it becomes a simpler expression,

$$H = e^{-\beta/2} \left(-\kappa a - \frac{P_a^2}{16a} - \frac{P_a P_\beta}{4a^2} + \frac{3P_\beta^2}{4a^3} \right) + a^{-3\alpha} e^{-\beta\alpha/2} P_T. \tag{12}$$

Here, P_T is the only remaining canonical variable associated with matter [61]. For simplicity, here we use the gauge $N = 1$.

3. The Noncommutative Bianchi Models for Any Perfect Fluid

We consider that the NC Hamiltonian has the same form as the commutative Hamiltonian (12). Our main motivation to write the NC Hamiltonian in the same form as the commutative one is simplicity. We believe that the introduction of other terms, not present in the commutative Hamiltonian, would be difficult to justify. It can be rewritten simply by placing the *nc* index in the commutative variables, which we call NC variables, to differentiate it from the old variables. As we write below,

$$H_{nc} = e^{-\beta_{nc}/2} \left(-\kappa a_{nc} - \frac{P_{a_{nc}}^2}{16 a_{nc}} - \frac{P_{a_{nc}} P_{\beta_{nc}}}{4 a_{nc}^2} + \frac{3P_{\beta_{nc}}^2}{4 a_{nc}^3} \right) + a_{nc}^{-3\alpha} e^{-\beta_{nc}\alpha/2} P_{T_{nc}}. \tag{13}$$

Here, $P_{a_{nc}}$, $P_{\beta_{nc}}$, $P_{T_{nc}}$ are, respectively, the canonically conjugated momenta to the coordinates a_{nc}, β_{nc}, T_{nc} in the NC model.

The NC model is particularly relevant for exploring the early universe, where quantum gravity effects could be significant [44]. In NC cosmology, it is assumed that some of the classical phase space variables do not commute, which introduces a modified algebra in this space [45,46,48,64]. For the present model, we introduce the following Poisson brackets (PBs):

$$\begin{aligned}&\{a_{nc},\ T_{nc}\} = \{\beta_{nc},\ T_{nc}\} = \{P_{a_{nc}},\ P_{T_{nc}}\} = \{P_{\beta_{nc}},\ P_{T_{nc}}\} = 0\\&\{a_{nc},\ \beta_{nc}\} = \{a_{nc},\ P_{\beta_{nc}}\} = \{\beta_{nc},\ P_{a_{nc}}\} = \{P_{a_{nc}},\ P_{\beta_{nc}}\} = 0\end{aligned} \tag{14}$$

$$\{a_{nc},\ P_{a_{nc}}\} = \{\beta_{nc},\ P_{\beta_{nc}}\} = \{T_{nc},\ P_{T_{nc}}\} = 1 \tag{15}$$

$$\{a_{nc},\ P_{T_{nc}}\} = \{\beta_{nc},\ P_{T_{nc}}\} = \{T_{nc},\ P_{a_{nc}}\} = \{T_{nc},\ P_{\beta_{nc}}\} = \gamma. \tag{16}$$

Here, γ is the NC parameter that should be a small, dimensionless quantity in our current universe. All effects resulting from noncommutativity are concentrated in this parameter. From a general point of view, the deformed Poisson brackets algebra introduces a modification in the phase space of theory. In particular, since Equation (16) are Poisson brackets between geometrical and matter phase space variables and momenta, we expect new physical phenomena appearing in the geometrical as well as matter sectors of the NC model. In the present paper, we investigate the modifications introduced in the dynamics of the model due to the presence of the NC parameter γ. More precisely, we want to know how the expansion of the universe is influenced by the NC structure. The main motivation for our choice of the commutation relations in Equation (16) is an extension of a previous choice made in Ref. [50]. It introduces a novelty in the part of the paper associated with the Bianchi I cosmological model, and it is, also, easier to compare.

Now, instead of working directly with the physical NC variables of the Hamiltonian (13), as a matter of simplicity, we introduce new auxiliary canonical variables $(a_c,\ \beta_c,\ T_c,\ P_{a_c},\ P_{\beta_c},\ P_{T_c})$, defined as

$$\begin{aligned}&a_{nc} \to a_c + (\gamma/2)T_c,\ \ P_{a_{nc}} \to P_{a_c} + (\gamma/2)P_{T_c},\\&T_{nc} \to T_c + (\gamma/2)a_c,\ \ P_{T_{nc}} \to P_{T_c} + (\gamma/2)P_{a_c},\\&\beta_{nc} \to \beta_c,\ \ P_{\beta_{nc}} \to P_{\beta_c}.\end{aligned} \tag{17}$$

Here, $(a_c,\ \beta_c,\ T_c)$ and $(P_{a_c},\ P_{\beta_c},\ P_{T_c})$ are new coordinates and momenta in a commutative phase space. They satisfy the usual commutative Poisson brackets: $\{a_c,\ P_{a_c}\} = \{\beta_c,\ P_{\beta_c}\} = \{T_c,\ P_{T_c}\} = 1$ and all other Poisson brackets are zero. It is possible to show that the new expressions of the NC variables, given in terms of the commutative variables and γ Equation (17), fully satisfy the Poisson brackets (14)–(16), up to the first order in γ. These transformations Equation (17) are also known as Bopp shifts [65]. This technique of Bopp shift transformations is particularly significant in cosmology, as it provides a method to incorporate noncommutativity into classical systems by modifying the phase space coordinates [45,64].

With the aid of the transformations Equation (17), we can rewrite the Hamiltonian (13) in terms of the new coordinates and momenta, up to the first order in γ, which gives us

$$\begin{aligned}H_c = e^{-\frac{\beta_c}{2}}\left(-\kappa\left(a_c + \frac{\gamma}{2}T_c\right) - \frac{\left(P_{a_c} + \frac{\gamma}{2}P_{T_c}\right)^2}{16\left(a_c + \frac{\gamma}{2}T_c\right)} - \frac{\left(P_{a_c} + \frac{\gamma}{2}P_{T_c}\right)P_{\beta_c}}{4\left(a_c + \frac{\gamma}{2}T_c\right)^2} + \frac{3P_{\beta_c}^2}{4\left(a_c + \frac{\gamma}{2}T_c\right)^3}\right)\\+\left(a_c + \frac{\gamma}{2}T_c\right)^{-3\alpha} e^{-\frac{1}{2}\beta_c\alpha}\left(P_{T_c} + \frac{\gamma}{2}P_{a_c}\right).\end{aligned} \tag{18}$$

Here, H_c represents the NC Hamiltonian, expressed in terms of the auxiliary commutative variables denoted by the subscript c.

The Hamiltonian formalism provides a framework that describes the time evolution of a system through Hamilton's equations. Using the Hamiltonian H_c (18), the equations of motion for the BI, KS, and BIII models are given by:

$$\dot{a}_c = \{a_c, H_c\} = -\frac{e^{-\frac{\beta_c}{2}} P_{a_c}}{8\left(a_c + \frac{\gamma}{2} T_c\right)} - \frac{e^{-\frac{\beta_c}{2}} P_{\beta_c}}{4\left(a_c + \frac{\gamma}{2} T_c\right)^2} - \frac{\gamma e^{-\frac{\beta_c}{2}} P_{T_c}}{16\left(a_c + \frac{\gamma}{2} T_c\right)} + \frac{1}{2}\gamma e^{-\frac{1}{2}\alpha\beta_c}\left(a_c + \frac{\gamma}{2} T_c\right)^{-3\alpha}, \tag{19}$$

$$\begin{aligned}\dot{P}_{a_c} = \{P_{a_c}, H_c\} = &-\frac{e^{-\frac{\beta_c}{2}} P_{a_c} P_{\beta_c}}{2\left(a_c + \frac{\gamma}{2} T_c\right)^3} - \frac{\gamma e^{-\frac{\beta_c}{2}} P_{a_c} P_{T_c}}{16\left(a_c + \frac{\gamma}{2} T_c\right)^2} - \frac{e^{-\frac{\beta_c}{2}} P_{a_c}^2}{16\left(a_c + \frac{\gamma}{2} T_c\right)^2} \\ &+ \frac{3}{2}\alpha\gamma P_{a_c} e^{-\frac{1}{2}\alpha\beta_c}\left(a_c + \frac{\gamma}{2} T_c\right)^{-3\alpha-1} - \frac{\gamma e^{-\frac{\beta_c}{2}} P_{\beta_c} P_{T_c}}{4\left(a_c + \frac{\gamma}{2} T_c\right)^3} \\ &+ \frac{9 e^{-\frac{\beta_c}{2}} P_{\beta_c}^2}{4\left(a_c + \frac{\gamma}{2} T_c\right)^4} + 3\alpha P_{T_c} e^{-\frac{1}{2}\alpha\beta_c}\left(a_c + \frac{\gamma}{2} T_c\right)^{-3\alpha-1} + \kappa e^{-\frac{\beta_c}{2}},\end{aligned} \tag{20}$$

$$\dot{\beta}_c = \{\beta_c, H_c\} = -\frac{e^{-\frac{\beta_c}{2}} P_{a_c}}{4\left(a_c + \frac{\gamma}{2} T_c\right)^2} + \frac{3 e^{-\frac{\beta_c}{2}} P_{\beta_c}}{2\left(a_c + \frac{\gamma}{2} T_c\right)^3} - \frac{\gamma e^{-\frac{\beta_c}{2}} P_{T_c}}{8\left(a_c + \frac{\gamma}{2} T_c\right)^2}, \tag{21}$$

$$\begin{aligned}\dot{P}_{\beta_c} = \{P_{\beta_c}, H_c\} = &-\frac{e^{-\frac{\beta_c}{2}} P_{a_c} P_{\beta_c}}{8\left(a_c + \frac{\gamma}{2} T_c\right)^2} - \frac{\gamma e^{-\frac{\beta_c}{2}} P_{a_c} P_{T_c}}{32\left(a_c + \frac{\gamma}{2} T_c\right)} + \frac{1}{4}\alpha\gamma P_{a_c} e^{-\frac{1}{2}\alpha\beta_c}\left(a_c + \frac{\gamma}{2} T_c\right)^{-3\alpha} \\ &- \frac{e^{-\frac{\beta_c}{2}} P_{a_c}^2}{32\left(a_c + \frac{\gamma}{2} T_c\right)} - \frac{\gamma e^{-\frac{\beta_c}{2}} P_{\beta_c} P_{T_c}}{16\left(a_c + \frac{\gamma}{2} T_c\right)^2} + \frac{3 e^{-\frac{\beta_c}{2}} P_{\beta_c}^2}{8\left(a_c + \frac{\gamma}{2} T_c\right)^3} \\ &+ \frac{1}{2}\alpha P_{T_c} e^{-\frac{1}{2}\alpha\beta_c}\left(a_c + \frac{\gamma}{2} T_c\right)^{-3\alpha} - \frac{1}{2}\kappa a_c e^{-\frac{\beta_c}{2}} - \frac{1}{4}\kappa\gamma e^{-\frac{\beta_c}{2}} T_c,\end{aligned} \tag{22}$$

$$\dot{T}_c = \{T_c, H_c\} = -\frac{\gamma e^{-\frac{\beta_c}{2}} P_{a_c}}{16\left(a_c + \frac{\gamma}{2} T_c\right)} - \frac{\gamma e^{-\frac{\beta_c}{2}} P_{\beta_c}}{8\left(a_c + \frac{\gamma}{2} T_c\right)^2} + e^{-\frac{1}{2}\alpha\beta_c}\left(a_c + \frac{\gamma}{2} T_c\right)^{-3\alpha}, \tag{23}$$

$$\begin{aligned}\dot{P}_{T_c} = \{P_{T_c}, H_c\} = &-\frac{\gamma e^{-\frac{\beta_c}{2}} P_{a_c} P_{\beta_c}}{4\left(a_c + \frac{\gamma}{2} T_c\right)^3} - \frac{\gamma e^{-\frac{\beta_c}{2}} P_{a_c}^2}{32\left(a_c + \frac{\gamma}{2} T_c\right)^2} + \frac{9\gamma e^{-\frac{\beta_c}{2}} P_{\beta_c}^2}{8\left(a_c + \frac{\gamma}{2} T_c\right)^4} \\ &+ \frac{3}{2}\alpha\gamma P_{T_c} e^{-\frac{1}{2}\alpha\beta_c}\left(a_c + \frac{\gamma}{2} T_c\right)^{-3\alpha-1} + \frac{1}{2}\kappa\gamma e^{-\frac{\beta_c}{2}}.\end{aligned} \tag{24}$$

To analyze the evolution of the universe, our goal is to solve the equations corresponding to the variables a_c, β_c, and T_c, which are related to the physical variables a_{nc} and β_{nc}, as mentioned earlier. To achieve this, it is necessary to rewrite the equations of motion derived from the Hamiltonian H_c, expressing them exclusively in terms of these variables and their time derivatives, thus eliminating explicit dependencies on the conjugate momenta. This approach simplifies the description of the dynamics of the system and makes it easier to analyze the impact of the corrections in γ on the evolution of the dynamic variables.

We observe that $\dot{P}_{T_c}$ Equation (24) is proportional to $\dot{P}_{a_c}$ Equation (20) with a factor of $\gamma/2$. This implies $\dot{P}_{T_c} = \frac{\gamma}{2}\dot{P}_{a_c}$. Integrating this equation, we obtain the following expression for the canonical momentum,

$$P_{T_c} = \frac{\gamma}{2} P_{a_c} + C. \tag{25}$$

where C is a positive integration constant that represents the initial energy density of the fluid. This constant is a quantity that is conserved during the evolution of the system and is determined by the initial conditions.

Also, if we choose (19) and (21) from the equations of motion above and combine them, with the aid of Equation (25), we may obtain the following expressions for canonical momenta P_{a_c} and P_{β_c},

$$\begin{aligned} P_{a_c} = & -3\gamma e^{\frac{\beta_c}{2}} T_c \dot{a}_c - 6a_c e^{\frac{\beta_c}{2}} \dot{a}_c - \gamma a_c e^{\frac{\beta_c}{2}} T_c \dot{\beta}_c - a_c^2 e^{\frac{\beta_c}{2}} \dot{\beta}_c \\ & + 3\gamma e^{\frac{\beta_c}{2} - \frac{1}{2}\alpha\beta_c} \left(a_c + \frac{1}{2}\gamma T_c \right)^{1-3\alpha} - \frac{C\gamma}{2}, \end{aligned} \tag{26}$$

$$\begin{aligned} P_{\beta_c} = & -\gamma a_c e^{\frac{\beta_c}{2}} T_c \dot{a}_c - a_c^2 e^{\frac{\beta_c}{2}} \dot{a}_c + \frac{3}{4}\gamma a_c^2 e^{\frac{\beta_c}{2}} T_c \dot{\beta}_c + \frac{1}{2} a_c^3 e^{\frac{\beta_c}{2}} \dot{\beta}_c \\ & + \frac{1}{2}\gamma e^{\frac{\beta_c}{2} - \frac{1}{2}\alpha\beta_c} \left(a_c + \frac{1}{2}\gamma T_c \right)^{2-3\alpha}. \end{aligned} \tag{27}$$

These equations express the canonical momenta P_{a_c} and P_{β_c} in terms of the variables a_c, β_c, T_c, and their time derivatives.

Now, substituting the canonical momenta P_{T_c}, P_{a_c}, and P_{β_c} from Equations (25)–(27) into the time evolution of the matter-associated variable Equation (23), we obtain the following expression for $\dot{T}_c$,

$$\dot{T}_c = \frac{1}{2}\gamma \dot{a}_c + e^{-\frac{1}{2}\alpha\beta_c} \left(a_c + \frac{1}{2}\gamma T_c \right)^{-3\alpha}. \tag{28}$$

This equation describes the variable $\dot{T}_c$ in terms of a_c, $\dot{a}_c$, and T_c, up to the first order in the NC parameter γ.

Next, it is necessary to derive $\dot{a}_c$ (19) and $\dot{\beta}_c$ (21) with respect to time. This process allows for obtaining second-order differential equations, which is important to fully describe the temporal evolution of the system's variables. Differential equations provide detailed information on how a_c and β_c evolve over time. Furthermore, deriving these expressions ensures a consistent physical description aligned with the system's initial conditions and constraints. These second derivatives are as follows:

$$\begin{aligned} \ddot{a}_c = & -\frac{3}{4}\gamma \dot{a}_c e^{-\frac{1}{2}\alpha\beta_c} \left(a_c + \frac{1}{2}\gamma T_c \right)^{-3\alpha-1} + \frac{3}{2}\alpha\gamma \dot{a}_c e^{-\frac{1}{2}\alpha\beta_c} \left(a_c + \frac{1}{2}\gamma T_c \right)^{-3\alpha-1} - \\ & \frac{\dot{a}_c^2}{2\left(a_c + \frac{1}{2}\gamma T_c \right)} + \frac{1}{8}\gamma e^{-\frac{1}{2}\alpha\beta_c} \dot{\beta}_c \left(a_c + \frac{1}{2}\gamma T_c \right)^{-3\alpha} + \frac{1}{4}\alpha\gamma e^{-\frac{1}{2}\alpha\beta_c} \dot{\beta}_c \left(a_c + \frac{1}{2}\gamma T_c \right)^{-3\alpha} \\ & - \frac{1}{8}\dot{\beta}_c^2 \left(a_c + \frac{1}{2}\gamma T_c \right) - \frac{1}{2}\alpha C e^{-\frac{1}{2}\alpha\beta_c - \frac{\beta_c}{2}} \left(a_c + \frac{1}{2}\gamma T_c \right)^{-3\alpha-2} - \frac{\kappa e^{-\beta_c}}{8\left(a_c + \frac{1}{2}\gamma T_c \right)} \\ & + \frac{\kappa a_c e^{-\beta_c}}{8\left(a_c + \frac{1}{2}\gamma T_c \right)^2} + \frac{\gamma\kappa e^{-\beta_c} T_c}{16\left(a_c + \frac{1}{2}\gamma T_c \right)^2} \end{aligned} \tag{29}$$

and

$$\begin{aligned} \ddot{\beta}_c = & -\frac{3\dot{a}_c \dot{\beta}_c}{a_c + \frac{1}{2}\gamma T_c} + \frac{3}{2}\gamma \dot{a}_c e^{-\frac{1}{2}\alpha\beta_c} \left(a_c + \frac{1}{2}\gamma T_c \right)^{-3\alpha-2} - \frac{\kappa e^{-\beta_c}}{4\left(a_c + \frac{1}{2}\gamma T_c \right)^2} - \frac{1}{2}\dot{\beta}_c^2 \\ & - \frac{5}{4}\gamma e^{-\frac{1}{2}\alpha\beta_c} \dot{\beta}_c \left(a_c + \frac{1}{2}\gamma T_c \right)^{-3\alpha-1} - \frac{3\kappa a_c e^{-\beta_c}}{4\left(a_c + \frac{1}{2}\gamma T_c \right)^3} - \frac{3\gamma\kappa e^{-\beta_c} T_c}{8\left(a_c + \frac{1}{2}\gamma T_c \right)^3} \end{aligned} \tag{30}$$

In this case, the derivatives of the canonical momenta $\dot{P}_{a_c}$ (20), $\dot{P}_{\beta_c}$ (22), $\dot{P}_{T_c}$ (24) and the conjugate canonical momenta P_{a_c} (26), P_{T_c} (25), P_{β_c} (27) were substituted.

The Hamiltonian H_c plays a crucial role as a constraint in the system $(H_c = 0)$, ensuring that the dynamic trajectories satisfy the equations of motion along with the physical conditions established by the model. By substituting the conjugate canonical momenta P_{a_c}(26), P_{T_c}(25), P_{β_c}(27) into the expression (18), we obtain

$$\begin{aligned} 0 = &-e^{\frac{\beta_c}{2}}\dot{a}_c\dot{\beta}_c\left(a_c+\frac{1}{2}\gamma T_c\right)^2 - 3e^{\frac{\beta_c}{2}}\dot{a}_c^2\left(a_c+\frac{1}{2}\gamma T_c\right) + \frac{1}{4}e^{\frac{\beta_c}{2}}\dot{\beta}_c^2\left(a_c+\frac{1}{2}\gamma T_c\right)^3 \\ &-\frac{1}{2}\gamma e^{\frac{\beta_c}{2}-\frac{1}{2}\alpha\beta_c}\dot{\beta}_c\left(a_c+\frac{1}{2}\gamma T_c\right)^{2-3\alpha} - 3\gamma\dot{a}_c e^{\frac{\beta_c}{2}-\frac{1}{2}\alpha\beta_c}\left(a_c+\frac{1}{2}\gamma T_c\right)^{1-3\alpha} \\ &+Ce^{-\frac{1}{2}\alpha\beta_c}\left(a_c+\frac{1}{2}\gamma T_c\right)^{-3\alpha} - \kappa e^{-\frac{\beta_c}{2}}\left(a_c+\frac{1}{2}\gamma T_c\right). \end{aligned} \tag{31}$$

This expression illustrates the dynamics dictated by the constraints of the Hamiltonian system, where the geometry of the universe (κ) and the corrections due to the NC parameter γ are incorporated within H_c.

4. Numerical Solution for a Radiation-Dominated Anisotropic Universe

From now on, we restrict our attention to the case of a radiation perfect fluid where $\alpha = 1/3$. The analytical solution of the coupled system of Equations (28)–(31) is unfeasible due to the nonlinearity of the terms in its variables for $\alpha = 1/3$. Therefore, we must solve it numerically. Furthermore, as mentioned above $\gamma \ll 1$. Then, using this property, in terms of the equations where γ appears in the denominator, a Taylor expansion is performed up to the first order in γ, which keeps all the γ's in the numerator. With these modifications, the system of equations and the Hamiltonian constraint are rewritten in such a way that they contain only terms up to the first order in γ, allowing for the determination of numerical solutions for the variables $a_c(t)$, $\beta_c(t)$, and $T_c(t)$. These equations are given by:

$$\begin{aligned} \ddot{a}_c = &-\frac{\dot{a}_c^2}{2a_c} - \frac{\gamma e^{-\frac{\beta_c}{6}}\dot{a}_c}{4a_c^2} + \frac{\gamma T_c\dot{a}_c^2}{4a_c^2} + \frac{5\gamma e^{-\frac{\beta_c}{6}}\dot{\beta}_c}{24a_c} - \frac{1}{8}a_c\dot{\beta}_c^2 + \frac{C\gamma e^{-\frac{1}{3}(2\beta_c)}T_c}{4a_c^4} - \frac{Ce^{-\frac{1}{3}(2\beta_c)}}{6a_c^3} \\ &-\frac{1}{16}\gamma T_c\dot{\beta}_c^2, \end{aligned} \tag{32}$$

$$\ddot{\beta}_c = -\frac{3\dot{a}_c\dot{\beta}_c}{a_c} + \frac{3\gamma T_c\dot{a}_c\dot{\beta}_c}{2a_c^2} + \frac{3\gamma e^{-\frac{\beta_c}{6}}\dot{a}_c}{2a_c^3} - \frac{5\gamma e^{-\frac{\beta_c}{6}}\dot{\beta}_c}{4a_c^2} - \frac{\kappa e^{-\beta_c}}{a_c^2} + \frac{\gamma\kappa e^{-\beta_c}T_c}{a_c^3} - \frac{1}{2}\dot{\beta}_c^2, \tag{33}$$

$$\dot{T}_c = \frac{e^{-\frac{\beta_c}{6}}}{a_c} + \frac{1}{2}\gamma\dot{a}_c - \frac{\gamma e^{-\frac{\beta_c}{6}}T_c}{2a_c^2}, \tag{34}$$

and the constraint $(H_c = 0)$ is:

$$\begin{aligned} 0 = &-a_c^2 e^{\frac{\beta_c}{2}}\dot{a}_c\dot{\beta}_c - \gamma a_c e^{\frac{\beta_c}{2}}T_c\dot{a}_c\dot{\beta}_c - 3\gamma e^{\frac{\beta_c}{3}}\dot{a}_c - \frac{3}{2}\gamma e^{\frac{\beta_c}{2}}T_c\dot{a}_c^2 - 3a_c e^{\frac{\beta_c}{2}}\dot{a}_c^2 - \frac{1}{2}\gamma a_c e^{\frac{\beta_c}{3}}\dot{\beta}_c \\ &+\frac{3}{8}\gamma a_c^2 e^{\frac{\beta_c}{2}}T_c\dot{\beta}_c^2 + \frac{1}{4}a_c^3 e^{\frac{\beta_c}{2}}\dot{\beta}_c^2 - \frac{C\gamma e^{-\frac{\beta_c}{6}}T_c}{2a_c^2} + \frac{Ce^{-\frac{\beta_c}{6}}}{a_c} - \kappa a_c e^{-\frac{\beta_c}{2}} - \frac{1}{2}\gamma\kappa e^{-\frac{\beta_c}{2}}T_c. \end{aligned} \tag{35}$$

This system of equations describes the temporal evolution of the commutative variables $a_c(t)$, $\beta_c(t)$, and $T_c(t)$. These variables are related to the physical variables, the scale factor $a_{nc}(t)$ and the anisotropy parameter $\beta_{nc}(t)$, according to the transformations in Equations (17). Furthermore, the equations are highly coupled and non-linear, with the

presence of terms involving γ, which adjust the effects of anisotropy and corrections to the expansion of the universe. The constraint $H_c = 0$ represents an additional condition that must be satisfied for the system to be consistent. In the rest of this section we numerically solve these Equations (32)–(35) for many different values of the parameters γ and C, we also tested different initial conditions and let them evolve for many different periods of time, both for $\kappa = -1$ and $\kappa = -0$. The results displayed in the following Figures and Tables are examples that show in a nice way the conclusions we obtained in our numerical studies.

4.1. For the Case of $\kappa = -1$

The system of Equations (32)–(35), corresponding to case $\kappa = -1$, which represents a BIII cosmological model with open spatial curvature, was numerically solved due to the intrinsic complexity of the expressions involved. To this end, the initial conditions $a_c(0)$, $\dot{a}_c(0)$, $\beta_c(0)$, $\dot{\beta}_c(0)$, and $T_c(0)$ were specified, along with the values of the NC parameter γ and the integration constant C. Then it was verified that these initial values satisfied the dynamical constraint $H_c = 0$, as required by the Hamiltonian formalism. This constraint must hold for all times t, ensuring the consistency of the system's evolution within the canonical framework.

In practice, the procedure was carried out by treating $\dot{\beta}_c(0)$ as a free variable while fixing the other parameters, adjusting its value so that Equation (35) was fulfilled. Alternatively, if $\dot{\beta}_c(0)$ was chosen instead as fixed, the constant C was determined accordingly to satisfy the constraint. The choice between treating C or $\dot{\beta}_c(0)$ as the adjustable parameter is arbitrary and does not affect the validity or generality of the numerical solution obtained.

The numerical solutions for the variables $a_c(t)$, $\beta_c(t)$, and $T_c(t)$ enable the reconstruction of the physical variables through the transformations defined in (17). These are the scale factor $a_{nc}(t) = a_c + (\gamma/2)T_c$, which characterizes the expansion of the universe, and the anisotropy parameter $\beta_{nc}(t) = \beta_c$, which encodes the anisotropic features present in the early stages of cosmic evolution. A detailed analysis of the behavior of these physical variables will be presented in the following sections. The graphs that we are going to present are examples that show the general behavior of the solutions in a clear way. In these examples, we choose the numerical values of the parameters and initial conditions to show the different behaviors in the clearest way.

4.1.1. Varying the NC Parameter γ

In Figure 1, an analysis of the effect of the NC parameter γ on the evolution of the scale factor $a_{nc}(t)$ and the anisotropy parameter $\beta_{nc}(t)$ is initiated. In Table 1, numerical data on its behavior at different time instants are presented, showing how the different values of γ influence the expansion of the universe and the stabilization of anisotropy in later times.

Specifically, with respect to the evolution of the scale factor $a_{nc}(t)$, we observe from Figure 1a that the solutions are always expansive. On the other hand, depending on the value of the NC parameter γ, we identify a subtle but noticeable effect. From Table 1, we observe that: for t =100,000, the scale factor reaches the value of 499.3741 when $\gamma = 0$, 553.1807 when $\gamma = -0.2$, and 473.9523 when $\gamma = 0.2$. These results indicate that a negative value of γ slightly increases the expansion, while a positive value of γ slightly reduces it. Therefore, the expansion rate is slightly more pronounced for negative values of γ, suggesting that the parameter influences the rate of growth of the universe.

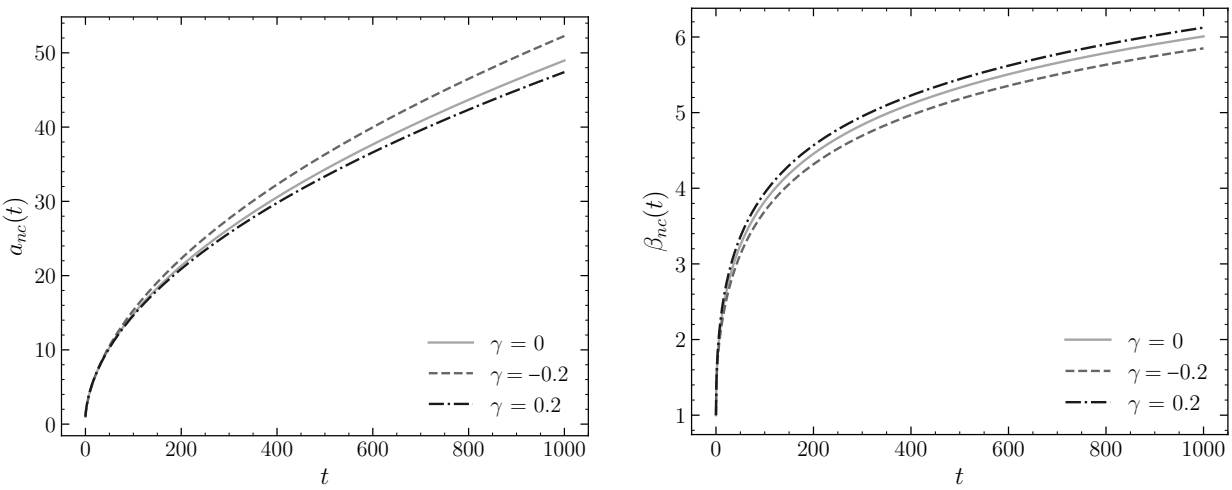

(**a**) (**b**)

Figure 1. The graphs (**a**,**b**) show the numerical solutions obtained under initial conditions: $a_c(0) = 1$, $\dot{a}_c(0) = 1$, $\beta_c(0) = 1$, $\dot{\beta}_c(0) = 1$, and $T_c(0) = 0$. For each selected value of $\gamma = \{0, -0.2, 0.2\}$, the corresponding value of $C = \{6.58747, 5.43337, 7.74158\}$ was calculated using the constraint $H_c = 0$, while keeping the other initial conditions fixed. Due to the *geometrized units* t is measured in centimeters. (**a**) Evolution of the scale factor $a_{nc}(t)$ as a function of time t. (**b**) Behavior of the anisotropy parameter $\beta_{nc}(t)$ as a function of time t.

Table 1. Results of the physical variables shown in Figure 1, for different time instances t, with $\gamma = 0$ in the upper part, $\gamma = -0.2$ in the central part, and $\gamma = 0.2$ in the lower part. Due to the *geometrized units* t is measured in centimeters.

t	$a_{nc}(t)$	$\beta_{nc}(t)$	$\dot{\beta}_{nc}(t)$
0	1	1	1
6765	129.164429	7.90581	0.000147
10,946	164.586699	8.386061	0.000091
17,711	209.632437	8.866669	0.000056
28,657	266.918407	9.347501	0.000035
46,368	339.773622	9.828475	0.000022
75,025	432.432997	10.309537	0.000013
100,000	499.374086	10.596825	0.000010
1,000,000	1580.695261	12.89924	9.999802×10^{-7}
0	1	1	1
6765	140.504186	7.724368	0.000146
10,946	179.714842	8.199524	0.00009
17,711	229.709761	8.675289	0.000056
28,657	293.446562	9.151532	0.000035
46,368	374.692907	9.628163	0.000021
75,025	478.247856	10.10512	0.000013
100,000	553.180714	10.390063	0.000010
1,000,000	1770.407126	12.676214	9.937651×10^{-7}
0	1	1	1
6765	123.850819	8.030033	0.000148
10,946	157.475065	8.51284	0.000092
17,711	200.172186	8.995896	0.000057
28,657	254.398652	9.479035	0.000035
46,368	323.278445	9.962151	0.000022
75,025	410.784542	10.445179	0.000013
100,000	473.952318	10.733554	0.000010
1,000,000	1491.833819	13.042393	0.000001

Regarding the anisotropy parameter $\beta_{nc}(t)$, we observe from Figure 1b that this parameter shows rapid growth in the initial stages, followed by stabilization toward a more stable value that varies with γ. From Table 1, we observe that: for $t = 100{,}000$, the obtained values are 10.60 for $\gamma = 0$, 10.39 for $\gamma = -0.2$, and 10.73 for $\gamma = 0.2$. These results show that a positive value of γ slightly increases the residual anisotropy, while a negative value of γ reduces it. Furthermore, the rate of change $\dot{\beta}_{nc}(t)$ decreases progressively over time, indicating that the anisotropy tends to a constant in the late-time regime. For $t = 100{,}000$, the values of $\dot{\beta}_{nc}(t)$ are 0.00001 for all cases, confirming that the evolution of anisotropy becomes practically negligible at late times, regardless of the value of γ.

4.1.2. Varying the Energy Density C

Next, the effect of varying the energy density C is studied. As shown in Figure 2a, an increase in C leads to a more accelerated growth of the scale factor $a_{nc}(t)$, indicating that a higher energy density in the system significantly influences the rate of expansion of the universe. This effect becomes particularly evident in later times, where the curves clearly separate and highlight a strong dependence of expansion on the value of C. Regarding the evolution of anisotropy $\beta_{nc}(t)$, we observe from Figure 2b that this parameter shows rapid growth in the early stages, followed by a smooth stabilization toward an asymptotic regime. Furthermore, as C increases, the value of anisotropy decreases.

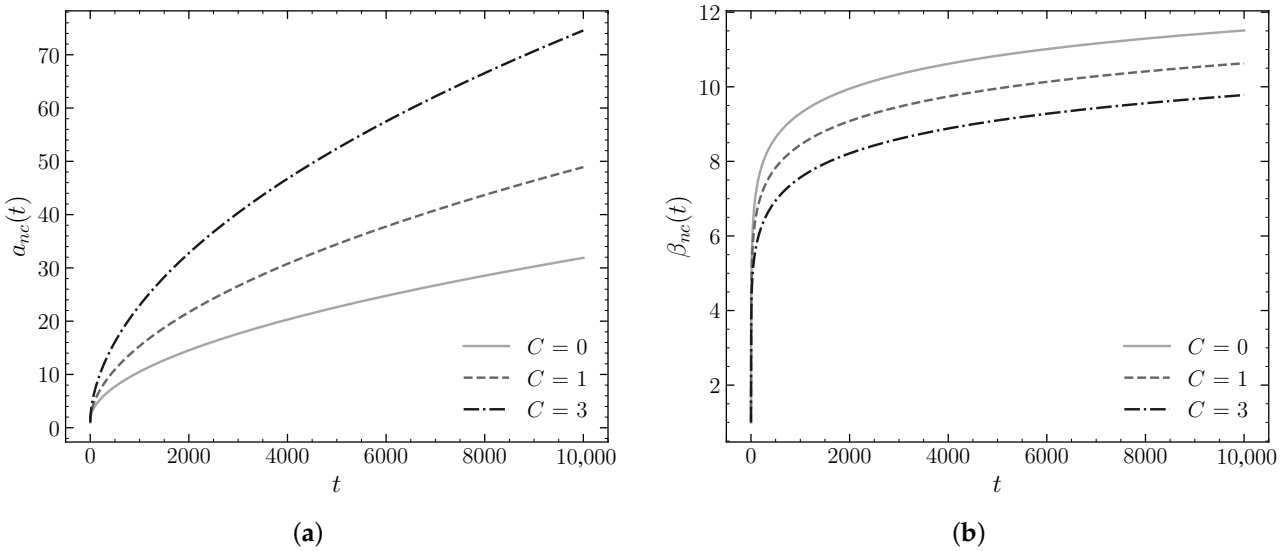

Figure 2. The graphs (**a**,**b**) show the numerical solutions obtained under initial conditions: $a_c(0) = 1$, $\dot{a}_c(0) = 1$, $\beta_c(0) = 1$, $T_c(0) = 0$, and the NC parameter $\gamma = -0.01$. For each selected value of $C = \{0, 1, 3\}$, the corresponding value of $\dot{\beta}_c(0) = \{5.78536, 5.50429, 4.8607\}$ was calculated using the constraint $H_c = 0$, while keeping the other initial conditions fixed. Due to the *geometrized units* t is measured in centimeters. (**a**) Evolution of the scale factor $a_{nc}(t)$ as a function of time t. (**b**) Behavior of the anisotropy parameter $\beta_{nc}(t)$ as a function of time t.

The numerical analysis presented in Table 2 shows that for $t = 100{,}000$, the scale factor reaches a value of 100.9551 when $C = 0$, and 238.6198 when $C = 3$, confirming that higher values of C significantly intensify the expansion of $a_{nc}(t)$. On the other hand, the anisotropy parameter $\beta_{nc}(t)$ tends to stabilize at finite values of 13.79 for $C = 0$ and 12.07 for $C = 3$, indicating that the anisotropy does not disappear, but its magnitude reduces as the energy density increases. Furthermore, the rate of change $\dot{\beta}_{nc}(t)$ decreases rapidly over time, reaching values on the order of 1.0×10^{-5} at $t = 100{,}000$ in both cases. This suggests that anisotropy evolves toward an equilibrium state as time progresses, although the value at which it stabilizes depends on the value of C.

Table 2. Results of the physical variables shown in Figure 2, for different time instances t, with $C = 0$ in the upper part and $C = 3$ in the lower part. Due to the *geometrized units* t is measured in centimeters.

t	$a_{nc}(t)$	$\beta_{nc}(t)$	$\dot{\beta}_{nc}(t)$
0	1	1	5.785361
6765	26.27245	11.128413	0.000144
10,946	33.34535	11.599695	0.00009
17,711	42.381682	12.073095	0.000056
28,657	53.915827	12.548111	0.000034
46,368	68.627935	13.024344	0.000021
75,025	87.383781	13.501489	0.000013
100,000	100.955147	13.786749	0.00001
1,000,000	321.134636	16.078007	9.964379×10^{-7}
0	1	1	4.860701
6765	61.116958	9.394866	0.000145
10,946	78.064725	9.868631	0.00009
17,711	99.641000	10.344768	0.000056
28,657	127.100693	10.822483	0.000035
46,368	162.041345	11.301244	0.000021
75,025	206.496301	11.7807	0.000013
100,000	238.619806	12.067232	0.00001
1,000,000	757.849614	14.366261	9.990592×10^{-7}

4.2. For the Case of $\kappa = 0$

In this case, the system of Equations (32)–(35) was solved for a BI cosmological model with no curvature, specifically $\kappa = 0$, using the same approach as in the previous subsection. The initial conditions $a_c(0)$, $\dot{a}_c(0)$, $\beta_c(0)$, $\dot{\beta}_c(0)$, and $T_c(0)$ were defined, together with the values of the parameters C and γ, to ensure that the restriction due to Equation (35) was satisfied. Based on the numerical solutions obtained for the commutative variables $a_c(t)$, $\beta_c(t)$, and $T_c(t)$, the physical variables related to the expansion of the universe, $a_{nc}(t) = a_c + \frac{\gamma}{2}T_c$, and the anisotropy parameter, $\beta_{nc}(t) = \beta_c$, were calculated. Then, a detailed analysis of these physical variables was carried out, including their asymptotic behavior and consistency with an isotropic radiation-dominated universe. The graphs that we are going to present are examples that show the general behavior of the solutions in a clear way. In these examples, we choose the numerical values of the parameters and initial conditions to show the different behaviors in the clearest way.

4.2.1. Varying the NC Parameter γ

To begin the analysis of the flat model ($\kappa = 0$), the impact of the NC parameter γ on the evolution of the scale factor $a_{nc}(t)$ and the anisotropy parameter $\beta_{nc}(t)$ is studied, as shown in Figure 3, along with the numerical results presented in Table 3. These results illustrate how different values of γ influence both the expansion rate of the universe and the stabilization of anisotropies at later times.

In particular, regarding the evolution of the scale factor $a_{nc}(t)$, it is observed that the presence of the NC parameter γ modifies the expansion dynamics of the universe. Although all cases show an accelerated growth, the expansion is more pronounced for $\gamma = -0.2$, while it is slightly smaller for $\gamma = 0.2$, compared to the commutative case $\gamma = 0$. From Table 3, we observe that for $t = 100{,}000$, the scale factor reaches a value of 408.3784 when $\gamma = 0$, 475.2813 for $\gamma = -0.2$, and 334.6021 for $\gamma = 0.2$. These results indicate that negative values of γ increase the expansion rate, while positive values tend to reduce it, confirming that the γ parameter has a significant effect on the evolution of $a_{nc}(t)$. The parameter

γ encapsulates geometric deformations that modify the dynamic equations of the early universe, affecting the expansion rate even in the absence of additional exotic components.

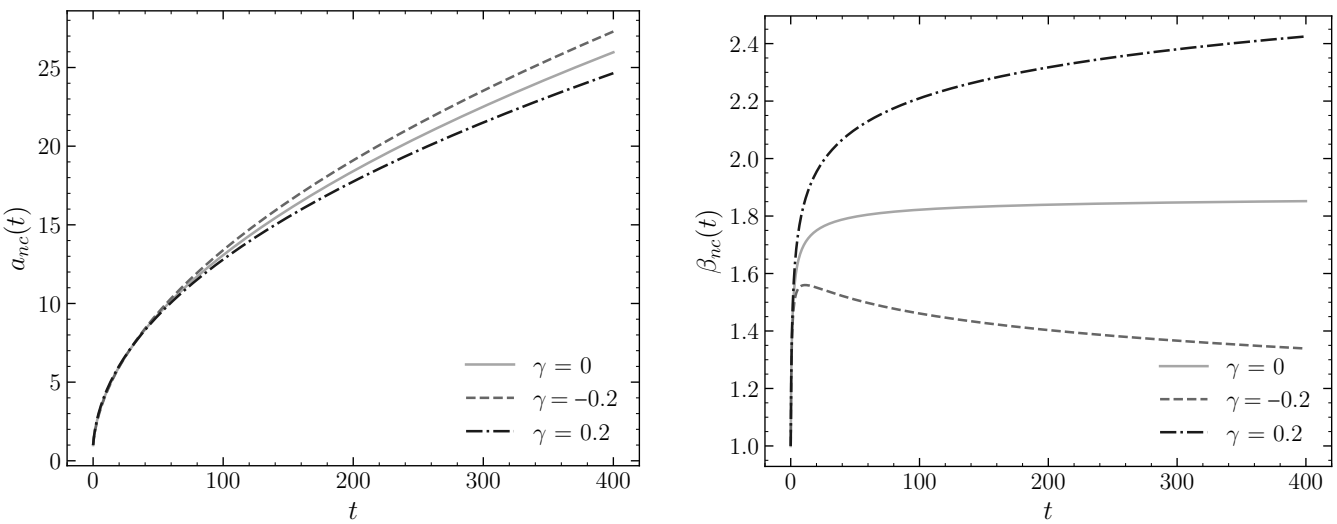

(**a**) (**b**)

Figure 3. The graphs (**a**,**b**) show the numerical solutions obtained under initial conditions: $a_c(0) = 1$, $\dot{a}_c(0) = 1$, $\beta_c(0) = 1$, $\dot{\beta}_c(0) = 1$, and $T_c(0) = 0$. For each selected value of $\gamma = \{0, -0.2, 0.2\}$, the corresponding value of $C = \{7.3040, 6.1499, 8.4581\}$ was calculated using the constraint $H_c = 0$, while keeping the other initial conditions fixed. Due to the *geometrized units* t is measured in centimeters. (**a**) Evolution of the scale factor $a_{nc}(t)$ as a function of time t. (**b**) Behavior of the anisotropy parameter $\beta_{nc}(t)$ as a function of time t.

Regarding the anisotropy parameter $\beta_{nc}(t)$, its behavior follows the expected pattern: rapid growth in the initial stages, followed by stabilization toward an asymptotic value. From Table 3, we observe that the final value of $\beta_{nc}(t)$ in $t = 100{,}000$ is approximately 1.88 for $\gamma = 0$, 0.76 for $\gamma = -0.2$, and 3.33 for $\gamma = 0.2$. This confirms that positive values of γ lead to higher residual anisotropy, while negative values favor greater isotropization.

Furthermore, the time derivative $\dot{\beta}_{nc}(t)$ decreases over time in all cases, confirming that the anisotropy tends to stabilize at late times. Again, from Table 3, we see that for $t = 100{,}000$, the values obtained are 9.4573×10^{-9} for $\gamma = 0$, -1×10^{-6} for $\gamma = -0.2$, and 2×10^{-6} for $\gamma = 0.2$. The lowest rate of change is observed in the commutative case, indicating that the anisotropy is nearly stabilized. In contrast, for $\gamma = \pm 0.2$, although the variation is small, anisotropy takes longer to reach its asymptotic state.

4.2.2. Varying the Energy Density C

Once the effect of the parameter γ has been explored, the impact of the energy density parameter C on the dynamics of the system is examined. As shown in Figure 4, a higher value of C increases the growth of the scale factor $a_{nc}(t)$, suggesting that the energy density of the system significantly influences the expansion rate of the universe. Regarding the evolution of the anisotropy parameter $\beta_{nc}(t)$, it shows rapid growth in the initial stages, followed by stabilization toward an asymptotic value, indicating that the universe reaches a more stable isotropic state after some time. Furthermore, as C increases, the asymptotic value of $\beta_{nc}(t)$ decreases.

Table 3. Results of the physical variables shown in Figure 3, for different time instances t, with $\gamma = 0$ in the upper part, $\gamma = -0.2$ in the central part, and $\gamma = 0.2$ in the lower part. Due to the *geometrized units* t is measured in centimeters.

t	$a_{nc}(t)$	$\beta_{nc}(t)$	$\dot{\beta}_{nc}(t)$
0	1	1	1
6765	106.317581	1.874408	5.374146×10^{-7}
10,946	135.200635	1.875963	2.611264×10^{-7}
17,711	171.940933	1.877186	1.268772×10^{-7}
28,657	218.675703	1.878147	6.164690×10^{-8}
46,368	278.123559	1.878902	2.995266×10^{-8}
75,025	353.742648	1.879496	1.455317×10^{-8}
100,000	408.37842	1.879789	9.457318×10^{-9}
1,000,000	1291.12363	1.881082	2.990694×10^{-10}
0	1	1	1
6765	117.819141	1.044834	−0.000016
10,946	151.162392	0.993182	−0.00001
17,711	193.944185	0.941453	−0.000006
28,657	248.83271	0.889743	−0.000004
46,368	319.249579	0.838128	−0.000002
75,025	409.58232	0.786664	−0.000001
100,000	475.281318	0.756025	−0.000001
1,000,000	1564.721984	0.513759	-1.037937×10^{-7}
0	1	1	1
6765	93.959956	2.87317	0.000024
10,946	117.941041	2.952831	0.000015
17,711	148.018844	3.033553	0.00001
28,657	185.734984	3.115385	0.000006
46,368	233.018627	3.198372	0.000004
75,025	292.283231	3.282557	0.000002
100,000	334.60206	3.333415	0.000002
1,000,000	986.042635	3.757939	1.912922×10^{-7}

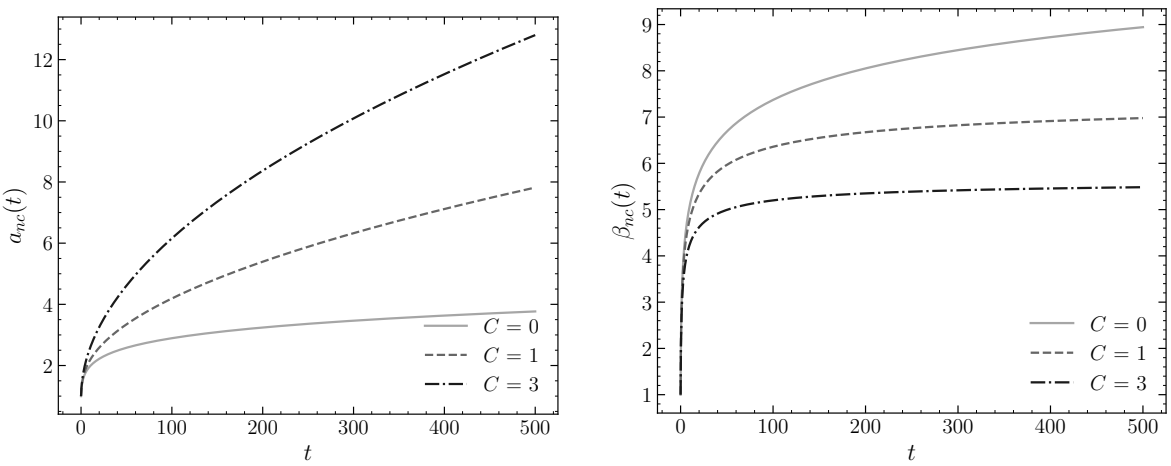

(**a**) (**b**)

Figure 4. The graphs (**a**,**b**) show the numerical solutions obtained under initial conditions: $a_c(0) = 1$, $\dot{a}_c(0) = 1$, $\beta_c(0) = 1$, $T_c(0) = 0$, and the NC parameter $\gamma = -0.01$. For each selected value of $C = \{0, 1, 3\}$, the corresponding value of $\dot{\beta}_c(0) = \{5.9746, 5.70785, 5.1066\}$ was calculated using the constraint $H_c = 0$, while keeping the other initial conditions fixed. Due to the *geometrized units* t is measured in centimeters. (**a**) Evolution of the scale factor $a_{nc}(t)$ as a function of time t. (**b**) Behavior of the anisotropy parameter $\beta_{nc}(t)$ as a function of time t.

The numerical analysis of these results, presented in Table 4, shows that for $t = 100{,}000$, the scale factor reaches a value of 12.8907 when $C = 0$, and 174.8610 when $C = 3$, confirming that higher values of C lead to a more pronounced expansion of the scale factor $a_{nc}(t)$. On the other hand, the anisotropy parameter $\beta_{nc}(t)$ tends to asymptotic values of 12.5 for $C = 0$ and 5.6 for $C = 3$, highlighting the influence of the energy density on the evolution of anisotropy. This behavior indicates that anisotropy does not disappear completely, but rather converges toward finite values in the asymptotic regime. Moreover, the time derivative of the anisotropy parameter, $\dot{\beta}_{nc}(t)$, decreases rapidly with time, reaching values on the order of 3.2134×10^{-7} for $C = 0$ and -9.1248×10^{-8} for $C = 3$. These results suggest that a higher energy density accelerates the isotropization process of the model, promoting a more efficient evolution toward a dynamic equilibrium state.

Table 4. Results of the physical variables shown in Figure 4, for different time instances t, with $C = 0$ in the upper part and $C = 3$ in the lower part. Due to the *geometrized units* t is measured in centimeters.

t	$a_{nc}(t)$	$\beta_{nc}(t)$	$\dot{\beta}_{nc}(t)$
0	1	1	5.974579
6765	5.825437	11.297205	0.000116
10,946	6.396436	11.654721	0.000063
17,711	7.129517	11.96011	0.000032
28,657	8.128739	12.198249	0.000015
46,368	9.52243	12.359923	0.000006
75,025	11.441132	12.446524	0.000001
100,000	12.890687	12.466424	3.213368×10^{-7}
1,000,000	38.00039	12.095334	-2.854031×10^{-7}
0	1	1	5.1066
6765	45.551467	5.630641	0.000003
10,946	57.857077	5.63739	9.368731×10^{-7}
17,711	73.537506	5.640777	2.296734×10^{-7}
28,657	93.51662	5.641516	-2.801714×10^{-8}
46,368	118.971422	5.640171	-9.993480×10^{-8}
75,025	151.401387	5.637187	-1.018942×10^{-7}
100,000	174.860954	5.634773	-9.124810×10^{-8}
1,000,000	555.70117	5.604837	-1.563588×10^{-8}

4.3. For the Case of $\kappa = +1$

In contrast to the solutions of the system of Equations (32)–(35) for $\kappa = 0$ and $\kappa = -1$, corresponding to the BI and BIII cosmological models, respectively, the solution for $\kappa = 1$, associated with the Kantowski-Sachs cosmological model, exhibits dynamic features of gravitational collapse. In particular, this model does not show sustained expansive behavior in its scale factor, and its anisotropy parameter does not tend toward isotropy in the asymptotic regime during the radiation era. For these reasons, the numerical analysis of the solution corresponding to $\kappa = 1$ falls outside the scope and interest of the present work, which focuses on models that tend toward isotropic and expansive evolution.

4.4. Influence of Spatial Curvature on NC Dynamics

Here, we compare how different spatial curvatures, specifically flat ($\kappa = 0$) and open ($\kappa = -1$) geometries, affect the evolution of the universe under the influence of a NC parameter γ. Both negative and positive values of γ are considered.

4.4.1. Case of Negative NC Parameter ($\gamma < 0$)

Following the detailed analysis of the cases with $\kappa = -1$ and $\kappa = 0$, presented in Sections 4.1 and 4.2, respectively, we now proceed to a direct comparison between both scenarios. This comparison focuses on the regime $\gamma < 0$, with the aim of clearly visualizing the dynamical differences induced by spatial curvature. In particular, the evolution of both the scale factor and the anisotropy parameter is evaluated together.

The results in Figure 5 indicate that the inclusion of a negative curvature improves the universe's expansion and substantially modifies the anisotropic behavior. The scale factor $a_{nc}(t)$ exhibits an accelerated growth in both cases, though with a significantly higher rate when $\kappa = -1$, suggesting that the open curvature acts as an amplifier of the expansive effect generated by noncommutativity. Meanwhile, the anisotropy parameter $\beta_{nc}(t)$, which tends to stabilize in the flat case, continues to grow under negative curvature, even at a decreasing rate. This behavior suggests that open geometry not only supports expansion but also delays the isotropization of the universe, extending the presence of anisotropies in the $\gamma < 0$ regime.

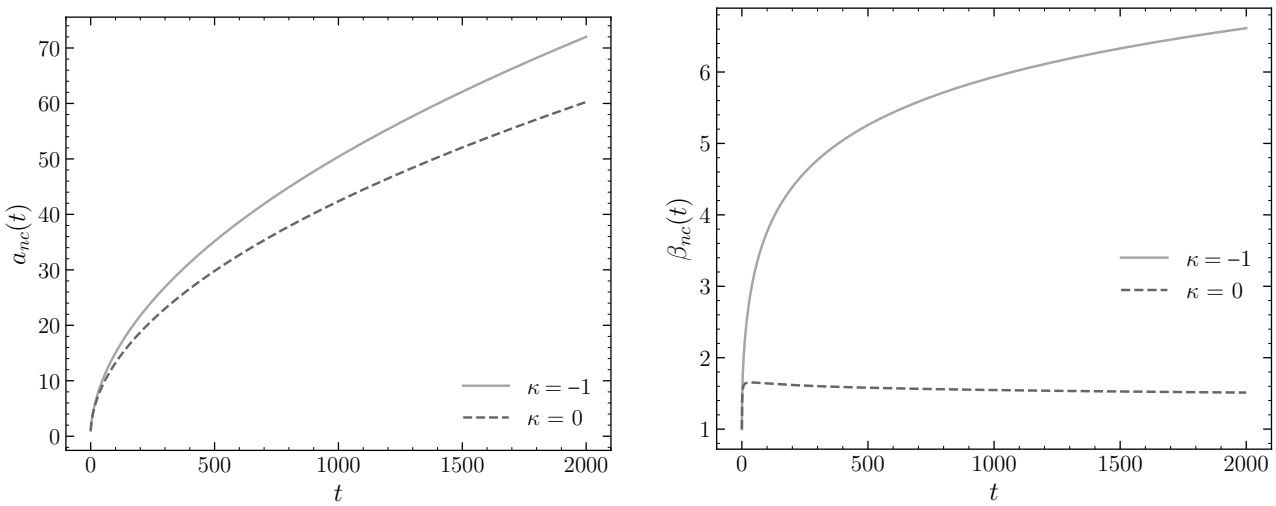

(**a**) (**b**)

Figure 5. The graphs (**a**,**b**) show the numerical solutions obtained under initial conditions: $a_c(0) = 1$, $\dot{a}_c(0) = 1$, $\beta_c(0) = 1$, $T_c(0) = 0$, $\dot{\beta}_c(0) = 1$ and the NC parameter $\gamma = -0.1$. For negative ($\kappa = -1$) and flat ($\kappa = 0$) geometry, the corresponding value of $C = \{6.0104, 6.7269\}$ was calculated using the constraint $H_c = 0$, while keeping the initial conditions fixed. Due to the *geometrized units* t is measured in centimeters. (**a**) Evolution of the scale factor $a_{nc}(t)$ as a function of time t. (**b**) Behavior of the anisotropy parameter $\beta_{nc}(t)$ as a function of time t.

4.4.2. Case of Positive NC Parameter ($\gamma > 0$)

After analyzing the dynamical behavior of the model for $\gamma > 0$ in Figure 6, it is observed that the inclusion of negative spatial curvature ($\kappa = -1$) continues to exert an amplifying effect on the expansion of the universe, although to a smaller extent than in the $\gamma < 0$ regime. The scale factor $a_{nc}(t)$ grows in both scenarios, but reaches significantly higher values in the presence of negative curvature, suggesting that this type of geometry improves the expansion rate even when the positive NC parameter tends to reduce it. On the other hand, the anisotropy parameter $\beta_{nc}(t)$ exhibits a notably different behavior in each case: while in the flat model ($\kappa = 0$) anisotropy stabilizes at late times, in the $\kappa = -1$ case it continues to grow, reaching much higher values. This result indicates that the combination of open geometry and noncommutativity with $\gamma > 0$ obstructs the isotropization process, prolonging the presence of anisotropies in the universe over time.

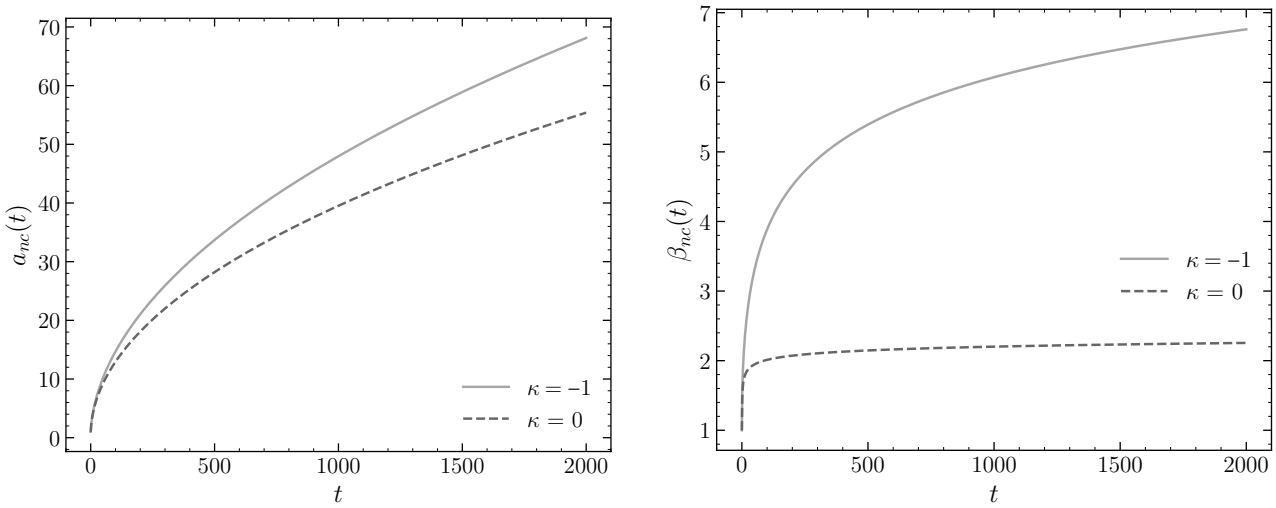

(**a**) (**b**)

Figure 6. The graphs (**a**,**b**) show the numerical solutions obtained under initial conditions: $a_c(0) = 1$, $\dot{a}_c(0) = 1$, $\beta_c(0) = 1$, $T_c(0) = 0$, $\dot{\beta}_c(0) = 1$ and the NC parameter $\gamma = 0.1$. For negative ($\kappa = -1$) and flat ($\kappa = 0$) geometry, the corresponding value of $C = \{7.1645, 7.8811\}$ was calculated using the constraint $H_c = 0$, while keeping the initial conditions fixed. Due to the *geometrized units* t is measured in centimeters. (**a**) Evolution of the scale factor $a_{nc}(t)$ as a function of time t. (**b**) Behavior of the anisotropy parameter $\beta_{nc}(t)$ as a function of time t.

5. Estimations of the NC Parameter γ Value with Observational Data

In this section, we estimate the value of the parameter γ using current observational data. This choice is motivated by the fact that it is easier to obtain good observational data of some cosmological parameters, needed for the estimations of γ, for the present age rather than the early age of the Universe. Therefore, we decided to compute the estimations of γ during the matter dominated universe. Another important motivation is that, during the matter dominated universe, we may assume that isotropization already took place, which simplifies the equations. To this end, we employ the NC Hamiltonian given in Equation (13) of the model corresponding to $\kappa = -1$, which describes an open universe in the context of Bianchi III. Our choice to consider a BIII instead of a BI model is due to the fact that, as far as we know, it is the first time the NC deformations of BIII cosmologies are explored. Initially, we assume the conditions of isotropy and homogeneity for the current Universe, implying that $\beta_{nc} \to$ constant and its associated canonical momentum $P_{\beta_{nc}} \to 0$. Within this framework, we consider that the observed accelerated expansion is entirely attributed to the presence of γ, which plays a crucial role in the dynamics of the Universe. Under these conditions, the NC Hamiltonian of the model reduces to

$$H_{nc} = -\kappa c^2 a_{nc} - \frac{P_{a_{nc}}^2}{16 a_{nc}} + a_{nc}^{-3\alpha} P_{T_{nc}}. \tag{36}$$

Unlike the previous sections, in this section we work directly with the physical variables, that is, the NC variables. This will allow us to determine the isotropic scale factor a_{nc} as a function of time. As mentioned above, in this section, we use conventional units to estimate the NC parameter γ.

Starting from the NC Hamiltonian in Equation (36), we calculate the dynamic equations using the deformed Poisson brackets described in Equations (14)–(16). These modified

brackets allow us to obtain the time evolution of the system's variables under the influence of noncommutativity. The resulting dynamic equations are:

$$\dot{a}_{nc} = \{a_{nc}, H_{nc}\} = -\frac{P_{a_{nc}}}{8a_{nc}} + \gamma a_{nc}^{-3\alpha}, \tag{37}$$

$$\dot{P}_{a_{nc}} = \{P_{a_{nc}}, H_{nc}\} = 3\alpha P_{T_{nc}} a_{nc}^{-3\alpha-1} - \frac{P_{a_{nc}}^2}{16a_{nc}^2} + \kappa c^2, \tag{38}$$

$$\dot{T}_{nc} = \{T_{nc}, H_{nc}\} = a_{nc}^{-3\alpha} - \frac{\gamma P_{a_{nc}}}{8a_{nc}}, \tag{39}$$

$$\dot{P}_{T_{nc}} = \{P_{T_{nc}}, H_{nc}\} = 3\alpha\gamma P_{T_{nc}} a_{nc}^{-3\alpha-1} - \frac{\gamma P_{a_{nc}}^2}{16a_{nc}^2} + \kappa c^2\gamma. \tag{40}$$

We can observe that Equations (38) and (40) are proportionally connected through the parameter γ. This connection is

$$\dot{P}_{T_{nc}} = \gamma \dot{P}_{a_{nc}}. \tag{41}$$

This expression can be easily integrated, resulting in

$$P_{T_{nc}} = \gamma P_{a_{nc}} + C_f, \tag{42}$$

where C_f is a constant related to the energy density of the fluid.

Since we are interested in deriving a dynamic equation for the scale factor a_{nc}, we can use Equation (37) to solve for $P_{a_{nc}}$, which leads us to

$$P_{a_{nc}} = -8a_{nc}\left(\dot{a}_{nc} - \gamma a_{nc}^{-3\alpha}\right). \tag{43}$$

Now, we impose the constraint $H_{nc} = 0$, which leads to Equation (36) being expressed as

$$-c^2\kappa a_{nc} - \frac{P_{a_{nc}}^2}{16a_{nc}} + a_{nc}^{-3\alpha} P_{T_{nc}} = 0. \tag{44}$$

Then, substituting the values of $P_{T_{nc}}$ and $P_{a_{nc}}$ given in Equations (42) and (43), we obtain

$$4\gamma^2 a_{nc}^{1-6\alpha} + C_f a_{nc}^{-3\alpha} - 4a_{nc}\dot{a}_{nc}^2 - \kappa c^2 a_{nc} = 0. \tag{45}$$

Furthermore, in the matter-dominated phase, the constant $\alpha = 0$, and the accelerated expansion is entirely due to the presence of the NC parameter γ. Thus, solving for $\dot{a}_{nc}$ from the previous equation with $\alpha = 0$, we obtain

$$\dot{a}_{nc} = \left(\frac{C_f}{4a_{nc}} - \frac{\kappa c^2}{4} + \gamma^2\right)^{1/2}. \tag{46}$$

From Equation (46), it is possible to determine a relationship between the NC scale factor a_{nc} and the age of the universe t. This is done by integrating the above equation from t^{eq} to t and a_{nc}^{eq} to a_{nc}, where the initial conditions t^{eq} and a_{nc}^{eq} represent, respectively, the age and the scale factor of the universe when the densities of matter and radiation were equal. The resulting relationship is

$$t = g^{-3/2} F(a_{nc}, C_f, \gamma) - g^{-3/2} F(a_{nc}^{eq}, C_f, \gamma) + t^{eq}, \tag{47}$$

with

$$F(a_{nc}, C_f, \gamma) = \sqrt{A + g\, a_{nc}}\sqrt{g\, a_{nc}} - A\, \ln\left(\frac{\sqrt{g\, a_{nc}} + \sqrt{A + g\, a_{nc}}}{\sqrt{A}}\right), \tag{48}$$

with $A = 4C_f$ and $g = -\kappa c^2/4 + \gamma^2$.

By comparing the Hubble function in the standard Friedmann–Robertson–Walker (FRW) cosmological model, given by $\dot{a} = H_0(\Omega_m/a - \kappa c^2/H_0^2)^{1/2}$, with Equation (46), we identify $C_f = 4\Omega_m H_0^2$ and $g = \Omega_k H_0^2/4 + \gamma^2$, $\Omega_k \equiv -\kappa c^2/H_0^2$ (c is the speed of light). Here, $\Omega_m = 0.315$ is the density parameter of matter, $\Omega_k = 0.001$ is the curvature parameter, $h = 0.674$, and $H_0 = (100\,h)$ km/s/Mpc $= 67.4$ km/s/Mpc is the Hubble constant. These values of the cosmological parameters were extracted from the 2018 Planck results [66]. It is known from the literature that local observations produce higher values of H_0 [67]. This fact is called the Hubble tension. Let us compute the γ estimates with the following higher value of the Hubble constant: $h = 0.733$, and $H_0 = 73.3$ km/s/Mpc [67]. The choice of these two values of H_0, will give an idea of how sensitive are the γ estimates with respect to the value of H_0.

To estimate the value of the NC parameter γ, it is necessary to provide the value of the scale factor $a_{nc}^{eq} = 4.15 \times 10^{-5}/(\Omega_m \mathrm{h}^2) = 2.90 \times 10^{-4}$ and the age of the universe $t^{eq} = 50.9$ Kyr corresponding to the epoch when the densities of matter and radiation were equal [68]. Additionally, the values of the scale factor at another moment in the history of the universe, a_{nc}, and the age of the universe $t(a_{nc})$ associated with that scale factor must also be provided. These will be determined using a "cosmological calculator" for an open-curvature universe ($\kappa = -1$) [69]. This "cosmological calculator" computes for given values of H_0, Ω_m, and the redshift z (or scale factor) the corresponding age of the universe, by solving a Friedmann equation for a FRW spacetime with $\kappa = -1$, coupled to a dust perfect fluid. The choice of considering an open-curvature FRW spacetime instead of a flat FRW spacetime, resulted in smaller values for the age of the universe for a given scale factor or redshift. In particular, for $a_{nc} = 1$ (or $z = 0$) the "cosmological calculator" gives $t_1(a_{nc} = 1) = 11.659$ Gyr (for $H_0 = 67.4$ km/s/Mpc) and $t_2(a_{nc} = 1) = 10.721$ Gyr (for $H_0 = 73.3$ km/s/Mpc), instead of the value $t(a_{nc} = 1) = 13.791$ Gyr, which would be obtained under the same conditions from a Friedmann equation for a flat FRW spacetime. Finally, substituting these values into Equation (47), the estimated value of the NC parameter can be obtained for the model. In Table 5, we present the estimated values of γ.

Table 5. Numerical values of the scale factor a_{nc}, the cosmic age t, and the NC parameter γ. The pairs (t_1, γ_1) and (t_2, γ_2) correspond to $H_0 = 67.4$ km/s/Mpc [66] and $H_0 = 73.3$ km/s/Mpc [67], respectively. The comparison illustrates the sensitivity of the NC parameter to the choice of H_0 and its behavior throughout different epochs of cosmic evolution.

a_{nc}	t_1 (Years)	γ_1	t_2 (Years)	γ_2
1.00	11.659×10^9	5.7064×10^{-11}	10.721×10^9	6.2099×10^{-11}
0.90	10.220×10^9	5.7073×10^{-11}	9.398×10^9	6.2110×10^{-11}
0.80	8.808×10^9	5.7084×10^{-11}	8.100×10^9	6.2120×10^{-11}
0.70	7.428×10^9	5.7100×10^{-11}	6.831×10^9	6.2142×10^{-11}
0.60	6.087×10^9	5.7119×10^{-11}	5.598×10^9	6.2164×10^{-11}
0.50	4.794×10^9	5.7152×10^{-11}	4.409×10^9	6.2205×10^{-11}
0.40	3.563×10^9	5.7170×10^{-11}	3.276×10^9	6.2289×10^{-11}
0.30	2.412×10^9	5.7275×10^{-11}	2.218×10^9	6.2405×10^{-11}
0.20	1.374×10^9	5.7627×10^{-11}	1.264×10^9	6.2717×10^{-11}
0.10	0.511×10^9	5.8943×10^{-11}	0.470×10^9	6.4321×10^{-11}
0.05	0.185×10^9	6.5073×10^{-11}	0.171×10^9	6.6517×10^{-11}

In Table 5, it is observed that as the scale factor decreases to smaller values, the age of the Universe also decreases. Similarly, the parameter γ steadily increases with the decrease of a_{nc} and the age of the universe t. This behavior suggests that the NC effects represented by γ are more significant during the early stages of the evolution of the Universe and

decrease as the Universe expands. This result is exactly what we expected and can be qualitatively compared with other results already published in the literature [48–51]. It is also clear from Table 5 that the estimated values of γ increase with increasing H_0.

6. Discussion and Conclusions

The results obtained in this study provide a new perspective on the evolution of the universe in Bianchi I and Bianchi III cosmological models, incorporating an NC parameter γ. This parameter, which extends the classical geometry of phase space into an NC context, has a significant impact on the dynamics expansion of the universe. It is observed that, for $\gamma < 0$, the expansion of the universe is increased compared to the commutative case ($\gamma = 0$), while for $\gamma > 0$, the expansion is slightly reduced. This behavior can be attributed to the correction introduced by the term $\left(\frac{\gamma}{2}\right)T_c$ to the scale factor a_{nc}, which effectively modifies the value of the NC scale factor. Although this term does not represent a force in the physical sense, it reflects how the structure of the NC phase space alters the geometry and, therefore, the dynamics of the expansion. Thus, in the context of the model, the negative values of γ tend to amplify the expansion, while positive values attenuate it, suggesting that the effects of noncommutativity can significantly influence cosmic evolution without resorting to additional exotic energy terms.

This finding suggests that the NC model could be a viable alternative to the cosmological constant Λ, as both parameters have similar effects on the expansion of the universe, although with important differences in their dynamics. In particular, the presence of γ significantly affects the temporal evolution of the anisotropy $\beta_{nc}(t)$. In the flat curvature model (Bianchi I), γ favors the isotropization of the universe, which is comparable to the behavior observed with a positive cosmological constant ($\Lambda > 0$). However, in the negative curvature model (Bianchi III), the anisotropy persists for a longer time, which could be explained by the influence of negative curvature, which slows down the isotropization of the universe.

The increase in energy density C also shows a more accelerated expansion of the universe, which is consistent with standard cosmological theory. Moreover, the estimated values of γ for a homogeneous and isotropic universe indicate that this parameter was more relevant in the early stages of the universe, matching the values predicted by previous studies. This behavior underscores the dynamic nature of noncommutativity in the cosmological context, especially in the early phases of the universe.

Regarding the estimation of γ, it was found that the current values of this parameter are small, with $a_{nc} = 1$, indicating that the influence of noncommutativity has diminished over time in a homogeneous and isotropic universe. However, the values of γ were slightly higher during the early stages of the universe, as shown in the simulated results. This behavior is expected, as noncommutativity should have had greater relevance in the early moments when the universe was denser and spatial scales were smaller. This 'evolution' of γ qualitatively agrees with the values estimated by other studies, reinforcing the validity of this model in describing the evolution of the early universe [48–51]. Another important result obtained from Table 5 is that the estimated values of γ increase with increasing H_0.

In conclusion, noncommutativity may provide a powerful tool for explaining cosmic acceleration and the early evolution of the universe, opening new avenues for understanding phenomena such as accelerated expansion and isotropization in different cosmological models. This study suggests that in certain contexts, noncommutativity could act as an alternative to the cosmological constant Λ, offering a distinct way of modelling the expansion of the universe in its early stages.

Author Contributions: Conceptualization, G.O.-N.; Methodology, G.O.-N.; Software, Y.S.A.; Validation, G.O.-N.; Formal analysis, G.O.-N.and Y.S.A.; Investigation, Y.S.A.; Data curation, Y.S.A.; Writing—original draft, Y.S.A.; Writing—review and editing, G.O.-N. and Y.S.A.; Supervision, G.O.-N. All authors have read and agreed to the published version of the manuscript.

Funding: This research was funded by Fundação de Amparo à Pesquisa do Estado de Minas Gerais (FAPEMIG), grant number APQ-06640-24.

Data Availability Statement: The original contributions presented in this study are included in the article. Further inquiries can be directed to the corresponding author.

Acknowledgments: Y. Soncco Apaza thanks Fundação de Amparo à Pesquisa do Estado de Minas Gerais (FAPEMIG) for his PhD scholarship. The authors thank the Federal University of Juiz de Fora (UFJF) for providing the academic environment and facilities that made this research possible.

Conflicts of Interest: The authors declare no conflicts of interest.

References

1. Rovelli, C. *Quantum Gravity*; Cambridge University Press: Cambridge, UK, 2004.
2. Wheeler, J.A. *Geometrodynamics and the Issue of the Final State*; Gordon and Breach: London, UK, 1964.
3. Mukhanov, V.F. *Physical Foundations of Cosmology*; Cambridge University Press: Cambridge, UK, 2005.
4. Weinberg, S. *Cosmology*; OUP Oxford: Oxford, UK, 2008.
5. Bianchi, L. Sugli spazi a tre dimensioni che ammettono un gruppo continuo di movimenti. *Mem. Mat. Fis. Della Soc. Ital. Delle Sci.* **1898**, *11*, 267352. English translation by Jantzen, R.T. On the three-dimensional spaces which admit a continuous group of motions. *Gen. Rel. Grav.* **2001**, *33*, 2171.
6. Jacobs, K.C. Bianchi Type I Cosmological Models. Ph.D. Thesis, California Institute of Technology, Pasadena, CA, USA, 1968.
7. Wald, R.M. Asymptotic behavior of homogeneous cosmological models in the presence of a positive cosmological constant. *Phys. Rev.* **1983**, *28*, 2118. [CrossRef]
8. Reis, S.C.d.; Shapiro, I.L. Cosmic anisotropy with reduced relativistic gas. *Eur. Phys. J. C* **2018**, *78*, 145. [CrossRef]
9. Oliveira-Neto, G.; Canedo, D.L.; Monerat, G.A. An Anisotropic Kantowski–Sachs Universe with Radiation, Dust and a Phantom Fluid. *Braz. J. Phys.* **2022**, *52*, 130. [CrossRef]
10. Oliveira, V.G.; de Oliveira Neto, G.; Shapiro, I.L. Kantowski–Sachs Model with a Running Cosmological Constant and Radiation. *Universe* **2024**, *10*, 83. [CrossRef]
11. Barrow, J.D.; Kodama, H. The isotropy of compact universes. *Class. Quantum Gravity* **2001**, *18*, 1753. [CrossRef]
12. Wainwright, J.; Ellis, G.F.R. *Dynamical Systems in Cosmology*; World Scientific: Singapore, 1997.
13. Heinzle, J.M.; Röhr, N.; Uggla, C. Matter and dynamics in closed cosmologies. *Phys. Rev. D* **2005**, *71*, 083506. [CrossRef]
14. Banerjee, A.; Duttachoudhury, S.B.; Sanyal, A.K. Bianchi type I cosmological model with a viscous fluid. *J. Math. Phys.* **1985**, *26*, 3010–3015. [CrossRef]
15. Balakin, A.B.; Zimdahl, W. Anisotropic cosmological models with nonminimally coupled magnetic field. *Phys. Rev. D* **2005**, *71*, 124014. [CrossRef]
16. Canfora, F.; Giacomini, A.; Pavluchenko, S.A. Cosmological dynamics of gravitating hadron matter. *Phys. Rev. D* **2014**, *90*, 043516. [CrossRef]
17. Kamenshchik, A.Y.; Pozdeeva, E.O.; Vernov, S.Y.; Starobinsky, A.A.; Tronconi, A.; Venturi, G. Induced gravity and minimally and conformally coupled scalar fields in Bianchi-I cosmological models. *Phys. Rev. D* **2018**, *97*, 023536. [CrossRef]
18. Casadio, R.; Kamenshchik, A.; Petriakova, P.; Mavrogiannis, P. Bianchi cosmologies, magnetic fields, and singularities. *Phys. Rev. D* **2023**, *108*, 023536. [CrossRef]
19. Bennet, C.L.; Hill, R.S.; Hinshaw, G.; Nolta, M.R.; Odegard, N.; Page, L.; Spergel, D.N.; Weiland, J.L. Astrophys. *J. Suppl. Ser.* **2003**, *148*, 97. [CrossRef]
20. Berera, A.; Buniy, R.V.; Kephart, T.W. The eccentric universe. *J. Cosmol. Astropart. Phys.* **2004**, *10*, 016. [CrossRef]
21. Gurzadyan, V.G.; Starobinsky, A.A.; Ghahramanyan, T.; Kashin, A.L.; Khachatryan, H.G.; Kuloghlian, H.; Vetrugno, D.; Yegorian, G. Large scale plane-mirroring in the cosmic microwave background WMAP5 maps. *Astron. Astrophys.* **2008**, *490*, 929. [CrossRef]
22. Gurzadyan, V.G.; Ghahramanyan, T.; Kashin, A.L.; Khachatryan, H.G.; Kocharyan, A.A.; Kuloghlian, H.; Vetrugno, D.; Yegorian, G. Plane-mirroring anomaly in the cosmic microwave background maps. *Astron. Astrophys.* **2009**, *498*, L1. [CrossRef]
23. Campanelli, L.; Cea, P.; Fogli, G.L.; Tedesco, L. Anisotropic dark energy and ellipsoidal Universe. *Int. J. Mod. Phys. D* **2011**, *20*, 1153. [CrossRef]

24. Russel, E.; Kilinc, C.B.; Pashev, O.K. Bianchi I model: An alternative way to model the present-day Universe. *Mon. Not. Roy. Astron. Soc.* **2014**, *442*, 2331. [CrossRef]
25. Schwarz, D.J.; Copi, C.J.; Hureter, D.; Starkman, G.D. CMB Anomalies after Planck. *Class. Quant. Grav.* **2016**, *33*, 184001. [CrossRef]
26. Buchert, T.; Coley, A.A.; Kleinert, H.; Roukema, B.F.; Wiltshire, D.L. Observational Challenges for the Standard FLRW Model. *Int. J. Mod. Phys. D* **2016**, *25*, 1630007. [CrossRef]
27. Tedesco, L. Ellipsoidal expansion of the Universe, cosmic shear, acceleration and jerk parameter. *Eur. Phys. J. Plus* **2018**, *133*, 188. [CrossRef]
28. Akarsu, O.; Kumar, S.; Sharma, S.; Tedesco, L. Constraints on a Bianchi type I spacetime extension of the standard CDM model. *Phys. Rev. D* **2019**, *100*, 023532. [CrossRef]
29. Ashtekar, A.; Wilson-Ewing, E. Loop quantum cosmology of Bianchi type I models. *Phys. Rev. D* **2009**, *79*, 083535. [CrossRef]
30. Bojowald, M. Loop quantum cosmology. *Living Rev. Relativ.* **2008**, *11*, 4. [CrossRef]
31. D'Eath, P.D. Quantization of the supersymmetric Bianchi-I model with a cosmological constant. *Phys. Lett. B* **1994**, *320*, 12–15. [CrossRef]
32. Alvarenga, F.G.; Batista, A.B.; Fabris, J.C.; Gonçalves, S.V.B. Troubles with Quantum Anisotropic Cosmological Models: Loss of Unitarity. *Gen. Rel. Grav.* **2003**, *35*, 1659. [CrossRef]
33. Guzmán, W.; Ortiz, C.; Sabido, M.; Socorro, J.; Aguero, M.A. Non-commutative Bianchi quantum cosmology. *Int. J. of Mod. Phys. D* **2007**, *16*, 1625–1632. [CrossRef]
34. Socorro, J.; Pimentel, L.O.; Ortiz, C.; Aguero, M. Scalar Field in the Bianchi I: Noncommutative Classical and Quantum Cosmology. *Int. J. Theor. Phys.* **2009**, *48*, 3567–3585. [CrossRef]
35. Socorro, J.; Rosales, J.J.; Sesma, L.T. Non-commutative classical and quantum fractionary cosmology: Anisotropic Bianchi type I case. *Gen. Relativ. Gravit.* **2025**, *57*, 23. [CrossRef]
36. Byland, S.; Scialom, D. Evolution of the Bianchi type I, Bianchi type III, and the Kantowski-Sachs universe: Isotropization and inflation. *Phys. Rev. D* **1998**, *57*, 6065. [CrossRef]
37. Pradhan, A.; Amirhashchi, H. Dark energy model in anisotropic Bianchi type-III space-time with variable EoS parameter. *Astrophys. Space Sci.* **2011**, *332*, 441–448. [CrossRef]
38. Mollah, M.R.; Singh, K.P.; Singh, P.S. Bianchi type-III cosmological model with quadratic EoS in Lyra geometry. *Int. J. Geom. Methods Mod. Phys.* **2018**, *15*, 1850194. [CrossRef]
39. Sahoo, P.K.; Sahu, S.K.; Nath, A. Anisotropic Bianchi-III cosmological model in f (R, T) gravity. *Eur. Phys. J. Plus* **2016**, *131*, 18. [CrossRef]
40. Christodoulakis, T.; Dimakis, N. Classical and quantum Bianchi type III vacuum Hořava–Lifshitz cosmology. *J. Geom. Phys.* **2012**, *62*, 2401–2413. [CrossRef]
41. Snyder, H.S. Quantized space-time. *Phys. Rev.* **1947**, *71*, 38. [CrossRef]
42. Seiberg, N.; Witten, E. String theory and noncommutative geometry. *J. High Energy Phys.* **1999**, *1999*, 032. [CrossRef]
43. Connes, A. *Noncommutative Geometry*; Academic Press: San Diego, CA, USA, 1994.
44. Douglas, M.R.; Nikita, A.N. Noncommutative field theory. *Rev. Mod. Phys.* **2001**, *73*, 977. [CrossRef]
45. Barbosa, G.D.; Pinto-Neto, N. Noncommutative geometry and cosmology. *Phys. Rev. D* **2004**, *70*, 103512. [CrossRef]
46. Bastos, C.; Bertolami, O.; Dias, N.C.; Prata, J.N. Phase-space noncommutative quantum cosmology. *Phys. Rev. D* **2008**, *78*, 023516. [CrossRef]
47. Ortiz, C.; Mena, E.; Sabido, M.; Socorro, J. (Non)commutative Isotropization in Bianchi I with Barotropic Perfect Fluid and Λ Cosmological. *Int. J. Theor. Phys.* **2008**, *47*, 1240–1251. [CrossRef]
48. Oliveira-Neto, G.; Vaz, A.R. Noncommutative cosmological model in the presence of a phantom fluid. *Eur. Phys. J. Plus* **2017**, *132*, 131. [CrossRef]
49. Oliveira-Neto, G.; Oliveira-Neto, G.; Marcon, L.F. Complete noncommutativity in a cosmological model with radiation. *Eur. Phys. J. Plus* **2021**, *136*, 584. [CrossRef]
50. Oliveira-Neto, G.; Abreu, T.M. A noncommutative Bianchi I model with radiation. *Int. J. Mod. Phys. D* **2024**, *33*, 2450112 . [CrossRef]
51. Abreu, T.M.; Oliveira-Neto, G.; Mendes, A.C.R.; Reis, S.C. Noncommutative effects in Bianchi I cosmology with reduced relativistic gas. *Class. Quantum Grav.* **2025**, *42*, 185010. [CrossRef]
52. Kantowski, R.; Sachs, R.K. Some spatially homogeneous anisotropic relativistic cosmological models. *J. Math. Phys.* **1966**, *7*, 443–446. [CrossRef]
53. Demianski, M. *Physics of the Expanding Universe: Cracow School on Cosmology*; Jodłowy Dwór, Poland, September 1978 (Lecture Notes in Physics, Volume 109); Springer: Berlin/Heidelberg, Germany, 1979.
54. Lorenz, D. Kantowski-Sachs cosmological solution with torsion. *J. Phys. A Math. Gen.* **1982**, *15*, 2809. [CrossRef]

55. Akarsu, O.; Kılınç, C.B. LRS Bianchi type I models with anisotropic dark energy and constant deceleration parameter. *Gen. Relativ. Gravit.* **2010**, *42*, 119–140. [CrossRef]
56. Camci, U.; Yildirim, A.; Oz, I.B. New exact solutions of Bianchi I, Bianchi III and Kantowski–Sachs spacetimes in scalar-coupled gravity theories via Noether gauge symmetries. *Astropart. Phys.* **2016**, *76*, 29–37. [CrossRef]
57. Misner, C.W. Minisuperspace. In *Magic Without Magic. JA Wheeler 60th Anniversary Volume*; Klauder, J., Ed.; W. H. Freeman and Co.: San Francisco, CA, USA, 1972; pp. 441–473.
58. Misner, C.W.; Thorne, K.S.; Wheeler, J.A. *Gravitation*; W. H. Freeman and Company: New York, NY, USA, 1973.
59. Ellis, G.F.R. Cosmological Models. In *Modern Cosmology*; Bonometto, S., Gorini, V., Moschella, U., Eds.; Institute of Physics Publishing: Bristol, UK; Philadelphia, PA, USA, 2002; pp. 108–158.
60. Schutz, B.F., Jr. Perfect fluids in general relativity: Velocity potentials and a variational principle. *Phys. Rev. D* **1970**, *2*, 2762. [CrossRef]
61. Alvarenga, F.G.; Fabris, J.C.; Lemos, N.A.; Monerat, G.A. Quantum cosmological perfect fluid models. *Gen. Relativ. Gravit.* **2002**, *34*, 651–663. [CrossRef]
62. Hawking, S.; Israel, W. General relativity: An Einstein centenary survey. In *General Relativity: An Einstein Centenary Survey*; Cambridge University Press: Cambridge, UK, 2010.
63. Lapchinskii, V.G.; Rubakov, V.A. Quantum gravitation: Quantization of the Friedmann model. *Teor. Mat. Fiz.* **1977**, *33*, 364–376. [CrossRef]
64. Socorro, J.; Rosales, J.J.; Toledo-Sesma, L. Non-commutative classical and quantum fractionary cosmology: FRW case. *Universe* **2024**, *10*, 192. [CrossRef]
65. Das, A.; Falomir, H.; Gamboa, J.; Mendez, F. Non-commutative supersymmetric quantum mechanics. *Phys. Lett. B* **2009**, *670*, 407–415. [CrossRef]
66. Aghanim, N. Planck 2018 results. VI. Cosmological parameters. Astron. *Astrophys* **2020**, *641*, A6 .
67. Wong, K.C.; Suyu, S.H.; Chen, G.C.; Rusu, C.E.; Millon, M.; Sluse, D.; Bonvin, V.; Fassnacht, C.D.; Taubenberger, S.; Auger, M.W.; et al. H0LiCOW-XIII. A 2.4 per cent measurement of H_0 from lensed quasars: 5.3 σ tension between early and late-Universe probes. *Mon. Not. Roy. Astron. Soc.* **2020**, *498*, 1420–1439. [CrossRef]
68. Dodelson, S.; Schmidt, F. *Modern Cosmology*; Academic Press: Cambridge, MA, USA, 2020.
69. Wright, E.L. A cosmology calculator for the world wide web. *Publ. Astron. Soc. Pac.* **2006**, *118*, 1711. [CrossRef]

Disclaimer/Publisher's Note: The statements, opinions and data contained in all publications are solely those of the individual author(s) and contributor(s) and not of MDPI and/or the editor(s). MDPI and/or the editor(s) disclaim responsibility for any injury to people or property resulting from any ideas, methods, instructions or products referred to in the content.